Arch Toxicol (2015) 89:459–483
DOI 10.1007/s00204-014-1264-0

BIOLOGICALS

Mechanisms of acute kidney injury induced by experimental *Lonomia obliqua* envenomation

Markus Berger · Lucélia Santi · Walter O. Beys-da-Silva · Fabrício Marcus Silva Oliveira · Marcelo Vidigal Caliari · John R. Yates III · Maria Aparecida Ribeiro Vieira · Jorge Almeida Guimarães

Received: 19 January 2014 / Accepted: 15 April 2014 / Published online: 6 May 2014

Abstract *Lonomia obliqua* caterpillar envenomation causes acute kidney injury (AKI), which can be responsible for its deadly actions. This study evaluates the possible mechanisms involved in the pathogenesis of renal dysfunction. To characterize *L. obliqua* venom effects, we subcutaneously injected rats and examined renal functional, morphological and biochemical parameters at several time points. We also performed discovery-based proteomic analysis to measure protein expression to identify molecular pathways of renal disease. *L. obliqua* envenomation causes acute tubular necrosis, which is associated with renal inflammation; formation of hematic casts, resulting from intravascular hemolysis; increase in vascular permeability and fibrosis. The dilation of Bowman's space and glomerular tuft is related to fluid leakage and intra-glomerular fibrin deposition, respectively, since tissue factor procoagulant activity increases in the kidney. Systemic hypotension also contributes to these alterations and to the sudden loss of basic renal functions, including filtration and excretion capacities, urinary concentration and maintenance of fluid homeostasis. In addition, envenomed kidneys increase the expression of proteins involved in cell stress, inflammation, tissue injury, heme-induced oxidative stress, coagulation and complement system activation. Finally, the localization of the venom in renal tissue agrees with morphological and functional alterations, suggesting also a direct nephrotoxic activity. In conclusion, the mechanisms of *L. obliqua*-induced AKI are complex involving mainly glomerular and tubular functional impairment and vascular alterations. These results are important to understand the mechanisms of renal injury and may suggest more efficient ways to prevent or attenuate the pathology of *Lonomia*'s envenomation.

Keywords Venom · *Lonomia* · Renal · Acute kidney injury · Nephrotoxicity · Acute tubular necrosis

Electronic supplementary material The online version of this article (doi:10.1007/s00204-014-1264-0) contains supplementary material, which is available to authorized users.

M. Berger · J. A. Guimarães (✉)
Laboratório de Bioquímica Farmacológica, Centro de Biotecnologia, Universidade Federal do Rio Grande do Sul (UFRGS), Av. Bento Gonçalves, 9500, CEP 91501-970 Porto Alegre, RS, Brazil
e-mail: guimar@cbiot.ufrgs.br

L. Santi · W. O. Beys-da-Silva · J. R. Yates III
Department of Chemical Physiology, The Scripps Research Institute, La Jolla, CA, USA

F. M. S. Oliveira · M. V. Caliari
Laboratório de Protozooses, Departamento de Patologia Geral, Instituto de Ciências Biológicas, Universidade Federal de Minas Gerais (UFMG), Belo Horizonte, MG, Brazil

M. A. R. Vieira
Laboratório de Fisiologia Renal, Departamento de Fisiologia e Biofísica, Instituto de Ciências Biológicas, Universidade Federal de Minas Gerais (UFMG), Belo Horizonte, MG, Brazil

Introduction

Accidents caused by venomous animals (mainly snakes, spiders, scorpions, bees, wasps and caterpillars) are a costly and critically important public health problem. Despite of this, public health authorities, nationally and internationally, have given little attention to this problem worldwide (Warrell 2010; Williams et al. 2010). Consequentially, the morbidity and mortality associated with envenomation cases produce a great impact on the population and health-care systems. One of the most important and lethal effects

of these animal venoms is nephrotoxicity, and a broad clinical spectrum of renal function impairment has been reported in human and experimental models of envenomation (Sitprija 2006; Berger et al. 2012). As kidneys are highly vascularized organs and have the ability to concentrate substances into urine, they are particularly susceptible to venom toxins. The most common clinical renal manifestation seen in human patients is acute tubular necrosis, but all renal structures may be involved. Thus, the occurrences of acute tubulointerstitial nephritis, renal cortical necrosis, mesangiolysis, vasculitis, glomerulonephritis, proteinuria, hematuria, hemoglobinuria and myoglobinuria have also been described (Sitprija 2006).

Lonomia obliqua caterpillars are well known in southern Brazil where they cause severe hemorrhagic syndrome characterized by perturbed coagulation, ecchymosis, acute kidney injury (AKI) and generalized hemorrhage. Since the 1980s, there has been a considerable increase in the number of hemorrhagic incidents in rural areas of the southernmost Brazilian states of Rio Grande do Sul, Santa Catarina and Paraná. The origin of this epidemic is not clear, but can be partially attributed to recent deforestation, as well as to a progressive reduction in the number of natural predators. Usually, accidents occur when the victim unknowingly leans against a tree trunk containing hundreds of caterpillars and comes into contact with the caterpillar's venomous bristles, which are chitinous evaginations of cuticule. Often, the caterpillar is crushed, the bristles are broken and venomous secretions, including hemolymph, penetrate the human skin (Veiga et al. 2001). The venom is composed of several active constituents with procoagulant, fibrinogenolytic, proteolytic and hemolytic activities (Pinto et al. 2010). Although consumptive coagulopathy secondary to intravascular disseminated coagulation is commonly observed in human and experimental animals, AKI is the leading cause of death from *L. obliqua* envenomation (Zannin et al. 2003; Gamborgi et al. 2006; Berger et al. 2010).

Early in the 1980s, the first registered cases of *L. obliqua*-induced hemorrhagic syndrome indicated that 18 % of envenomed patients had developed AKI. The mortality rate in these patients reached 50 % (Duarte et al. 1990, 1994). However, a lower incidence (5.2 %) was observed in the Brazilian state of Rio Grande do Sul from 1989 to 1995, when only 15 of 286 envenomed patients developed AKI (Duarte 1997). Another study analyzing a larger group of 2,067 envenomed patients in the Santa Catarina state in Brazil (from 1989 to 2003) reported that 39 victims (1.9 %) developed AKI (with serum creatinine levels $\geq$1.5 mg/dL). Eleven (32 %) of these patients were treated with dialysis and four (10.3 %) developed chronic renal injury (CRI). All victims with AKI presented concomitantly coagulation disturbances and hematuria and/or hemoglobinuria. Seven deaths (4 %) occurred during this period (Gamborgi et al. 2006). An important conclusion of this work is that, even after the introduction of antivenom therapy (with antilonomic serum) in 1995, there was no reduction in the incidence of AKI, despite the significant decrease in the number of deaths and patients who developed CRI (Gamborgi et al. 2006). In fact, recently, we observe that antivenom treatment was able to reduce creatinine and urea levels of rats only if administered 2 h post-venom injection. Serotherapy after 6 h of envenomation fails to neutralize the rising in biochemical markers of renal injury (Berger et al. 2013). Since the average time elapsed between the contact of a person with caterpillars and an appropriate medical care can vary from 19 to 37 h (Zannin et al. 2003), it seems imperative to achieve a better understanding of the mechanisms involved in venom-induced AKI. It is clear that having such knowledge available, it will then make possible to develop new efficient treatments in order to avoid or at least to reduce the progression of renal disease in *Lonomia*'s and other kind of animal envenoming.

The risk of conducting early renal biopsies in human patients, due to coagulation disturbances inherent to the envenomation, has made it difficult to analyze the acute kidney pathological alterations. There are only two case reports in the literature describing alterations of *Lonomia*-induced AKI. The main findings were oliguria, high levels of serum creatinine, thickening of the Bowman's capsule, focal tubular atrophy and acute tubular necrosis (Burdmann et al. 1996; Fan et al. 1998). Since no experimental studies were available until now, the contribution of several factors possibly associated with AKI, such as hemodynamic changes, vascular permeability alterations, hemolysis, tubular obstruction, glomerular fibrin deposition and even a direct venom nephrotoxicity, remains obscure in *Lonomia*-induced AKI.

In an attempt to better understand the progression of renal disease commonly observed after the contact with *L. obliqua* caterpillars, we have focused on the action of venom in the kidney. Therefore, an experimental rat model was used in order to characterize changes in renal function, tubular hydroelectrolytic transport, histopathology and hemodynamics.

Materials and methods

Reagents

Evans blue dye, purified coagulation factors (VII, IX and X) and molecular weight standards used in SDS-PAGE and Western blot were purchased from Sigma-Aldrich (Saint Louis, MO, USA). Chromogenic substrate for factor Xa (S2222, Bz-Ile-Glu-Gly-Arg-pNa) was obtained from Chromogenix (Milano, Italy). Ketamine and xylazine were

from Syntec, São Paulo, Brazil. *L. obliqua* antivenom (antilonomic serum—ALS), provided by the Butantan Institute (São Paulo, Brazil), was used as primary antibody for the detection of toxins in urine and renal tissue. ALS is a horse-derived concentrate of purified polyclonal antibodies (IgG) that had been raised against *L. obliqua* bristle extract (Rocha-Campos et al. 2001). Non-specific background staining in immunohistochemical reactions was blocked using Ultra V Block reagent (Thermo Fisher Scientific, Waltham, MA, USA).

Venom

Lonomia obliqua caterpillars were kindly provided by the Centro de Informações Toxicológicas (CIT), Porto Alegre, Rio Grande do Sul, Brazil. The specimens used in this study were collected in the cities of Bom Princípio and Progresso, both located in Rio Grande do Sul, Brazil. *L. obliqua* venom was obtained by homogenizing the bristles in cold phosphate buffered saline (PBS), pH 7.4, as previously described (Berger et al. 2010). The venom obtained following this procedure was designated as *L. obliqua* bristle extract (LOBE). The protein content of the LOBE samples was determined using a BCA assay kit (Pierce, Rockford, USA), and the aliquots were stored at −80 °C prior to use. The total number of caterpillars used for bristle extract preparation was 124 specimens, and the protein concentration of the LOBE samples was 4.10 mg/mL. The total amount of venom extracted per caterpillar was 2.4 mg. All of the LOBE samples had similar in vitro procoagulant activities, and the protein pattern for each sample as monitored by SDS-PAGE and gel filtration chromatography (Pinto et al. 2006; Berger et al. 2010) was also similar.

Ethical statements

All procedures involving animals were carried out in accordance with the Guiding Principles for the Use of Animals in Toxicology (International Society of Toxicology, http://www.toxicology.org) and the Brazilian College of Animal Experimentation (COBEA). The experimental protocol was approved by the ethical committee on research animal care of the Federal University of Rio Grande do Sul, Brazil (register number 2008177/2009), and by the Institute's Animal Ethics Committee of the Federal University of Minas Gerais, Brazil (protocol 177/2008).

Experimental protocol

Animals

Adult male Wistar rats, weighing 250–300 g, were supplied by the central animal facility of our institution. They were housed in standard conditions within a temperature controlled room (22–23 °C, on a 12-h light/dark cycle, with the lights on at 7:00 am) and had free access to water and food.

Selection of the venom dose

The severity of the natural envenoming is related mainly to the number of caterpillars involved as well as to the intensity of the exposure, since the venom is present not only in the caterpillar's bristles but also in their skin and hemolymph (Veiga et al. 2001). Considering that accidents with medical importance involve contact with a colony containing at least 40 to 50 caterpillars (Gamborgi et al. 2006) and that during venom extraction, after removal of all spicules, each caterpillar produces approximately 2.4 mg of venom, the total amount of venom injected in an individual weighing 70 kg can reach up to 1.4–1.7 mg/kg. In fact, these doses were calculated based on an artificial method of venom extraction, in which the caterpillar's bristle was macerated in a solution buffer. Thus, in a real envenomation situation, the total amount of venom transferred is probably lower than the amount calculated. In an attempt to reproduce the clinical conditions observed in a real envenomation, we selected doses of 1.0 and 1.5 mg/kg injected subcutaneously into rats. These doses were also in accordance with the amount of venom used in other studies to induce coagulopathy and test the efficacy of antilonomic serum (Berger et al. 2010; Dias da Silva et al. 1996; Rocha-Campos et al. 2001).

Venom administration

To follow the time course of kidney pathophysiological alterations, we used an experimental model of envenomation in rats. For this purpose, animals were divided into three groups ($n = 6$/group): The control animals (CTRL) were injected subcutaneously (s.c.) with 100 µL of sterile PBS solution and the experimental animals received a s.c injection containing 1.0 or 1.5 mg of LOBE per kg of body weight in a final volume of 100 µL. Immediately after treatments, the animals were distributed individually into metabolic cages, allowing quantitative urine collections and measurement of water intake. At several time points, post-venom injection (2, 6, 12, 24, 48 and 96 h), blood, urine and kidneys were obtained for biochemical, histopathological and immunohistochemical analyses.

Sample preparation

Blood was collected in conscious rats through the caudal vein in 1:10 (v/v) 3.8 % trisodium citrate. Plasma was obtained by centrifugation at 1,500×*g* for 10 min and stored at −80 °C prior to use. Urine samples were also

centrifuged at 2,500×*g* for 5 min, and the supernatants were stored at the same conditions. After blood collection, animals from the different groups were anesthetized by intraperitoneal (i.p.) injection of a mixture of ketamine (75 mg/kg) and xylazine (10 mg/kg). Then, an intracardiac perfusion was performed through the left ventricle with PBS solution, and a circulatory circuit was opened by an incision in the right atrium, to ensure the elimination of intravascular blood. Immediately after perfusion, kidneys were quickly removed. One of them was fixed for histological analysis and the other was frozen in liquid nitrogen and stored at −80 °C for the measurement of tissue factor activity and proteomic analysis.

Biochemical measurements

Urinary and plasma levels of creatinine, urinary γ-glutamyl transferase (γ-GT) activity and proteinuria were determined by spectrophotometry (Turner SP-830 plus Barnstead, Dubuque, Iowa, USA) using commercially available kits (BioClin/Quibasa, Belo Horizonte, Brazil). Plasma and urinary concentrations of Na^+ and K^+ were measured by flame photometry (CELM 180; Belo Horizonte, Minas Gerais, Brazil). Osmolality was determined in plasma and urine samples by cryoscopic osmometery using a Micro-Osmometer 3320 (Advanced Instruments, Norwood, Massachusetts, USA). Urine proteins were also analyzed by gel electrophoresis which was performed according to Laemmli (1970). Urine samples from animals of different times post-venom injection were diluted (10×) and aliquots of 10 µL were submitted to SDS-PAGE on 8–20 % gradient gels under reducing conditions. Toxins excreted in urine were detected by Western blot as previously described (Pinto et al. 2006). Aliquots containing 50 µg of protein were separated by SDS-PAGE and transferred to PVDF membranes. Toxins were recognized using as a primary antibody an equine anti-LOBE IgG (ALS) diluted 1:100 and as a secondary antibody a peroxidase-labeled anti-horse IgG diluted 1:1,000.

Renal function parameters

At the time intervals mentioned above, the following renal function parameters were determined: glomerular filtration rate (GFR), osmolar clearance (C_{osm}), water-free clearance (C_{H2O}), fractional water excretion (FE_{H2O}), fractional sodium excretion (FE^+_{Na}) and fractional potassium excretion (FE^+_K). GFR (expressed as mL/min/100 g of body weight) was estimated by the creatinine clearance (C_{cr}), using the standard formula: $C_{cr} = U_{cr}.\ V/P_{cr}$, where U_{cr} is the urinary creatinine concentration, V is the urinary output and P_{cr} is the plasma creatinine concentration. C_{osm} (expressed as mL/min) was calculated as $C_{osm} = U_{osm}/P_{osm}.\ V$, whereas U_{osm} and P_{osm} are the urinary and plasma osmolalities, respectively. Values of C_{H2O} (mL/min) and FE_{H2O} (%) were obtained, respectively, from the equations: $C_{H2O} = V - C_{osm}$ and $FE_{H2O} = V/GFR.100$. FE^+_{Na} and FE^+_K (expressed as %) were calculated according to the equation: FE = UE/PF.100. UE represents the urinary excretion of each ion, and PF is the amount filtered in plasma (both expressed as nmol/min).

Hemodynamic parameters

Systemic arterial pressure was measured in conscious rats by an indirect tail-cuff method using an electrosphygmomanometer (LE 5001, Harvard Apparatus, Holliston, Massachusetts, USA) combined with a pneumatic pulse transducer/amplifier, which provides output signals proportional to cuff pressure and amplified Korotkoff sounds. Three consecutive readings of mean arterial pressure and heart rate were recorded before blood collection for each animal in each time post-venom injection.

Renal vascular permeability

The extravasation of Evans blue dye into the kidney was used as an index of increased vascular permeability (Pompermayer et al. 2005). Rats received Evans blue dye (30 mg/kg) intravenously (1 mL/kg) via caudal vein 10 min prior to LOBE (1.5 mg/kg, s.c.) or PBS (100 µL, s.c.) injection. After 12 or 24 h, animals were anesthetized and perfused as described above to remove the intravascular Evans blue. Then, the kidneys were quickly removed, weighed and allowed to dry for 24 h at 40 °C. The dry weight was determined and Evans blue dye extracted in 2.5 mL of 1 % formamide (48 h at 40 °C). The absorbance of extracted solution was measured in triplicate using a microplate reader spectrophotometer (SpectraMAX, Molecular Devices Co., Sunnyvale, USA), and the amounts of Evans blue dye were calculated by a standard curve made with known concentrations of Evans blue. Results are presented as the amount of Evans blue dye extravasated (µg) per 100 mg of kidney tissue.

Renal tissue factor activity

Renal tissue factor (TF) was measured indirectly based on its ability to form a complex with factor VIIa (TF/FVIIa) to activate factor IX and X (Morrissey 1995). Briefly, the kidneys were collected as described above, homogenized in cold PBS solution containing 1 % Triton X-100 and centrifuged at 9,500×*g* for 15 min. Samples of supernatants (with 10 µg of protein) were incubated with a concentrate mixture of FVII + FIX + FX (total of 15 µg) in 20 mM Tris–HCl, pH 7.4 containing 10 mM of $CaCl_2$ for 10 min at

37 °C. Activated factor Xa (FXa) produced during the reaction was detected by the addition of a specific chromogenic substrate (0.2 mM S2222). The kinetics of *p*-nitroaniline release was monitored at 405 nm for 30 min in a final volume of 100 µL using a microplate reader spectrophotometer (SpectraMAX, Molecular Devices Co., Sunnyvale, USA). Each sample was measured in triplicate and results expressed as µmol of FXa generated per min per mg of kidney tissue.

Histology and immunohistochemistry

For renal histopathology, kidneys were collected as described above, sectioned sagitally and fixed in 10 % buffered formaldehyde, pH 7.2. After processing in alcohol and xylol, the organs were included in paraffin, and 4-µm-thick sections were obtained and stained with hematoxylin and eosin (H&E), periodic acid-Schiff (PAS) or picrosirius reagent.

For immunohistochemical analysis of venom distribution in renal tissue, the kidney sections were deparaffinized and treated with 10 % hydrogen peroxide solution in methanol for 15 min to block endogenous peroxidase activity. Non-specific binding sites were blocked with Ultra V Block reagent followed by incubation overnight at 4 °C with an equine anti-LOBE IgG (ALS) diluted 1:250 in PBS. After a washing step, the sections were incubated with the secondary antibody (a biotinylated anti-horse IgG produced in goat, diluted 1:100) and streptavidin diluted 1:100. The chromogenic reaction was developed by incubating the sections with 0.05 % diaminobenzidine solution and 0.2 % hydrogen peroxide. The progress of the reaction was monitored by light microscopy and stopped by washing the slides. Finally, the sections were counterstained with diluted Harris's hematoxylin. Control reactions were done by incubating kidney sections from non-envenomed rats with equine anti-LOBE IgG (ALS) under the same conditions as described above. No positive reactions were observed in these sections. Some sections were also used as negative controls. In these cases, the primary antibody was substituted by PBS.

Morphometric analysis

Glomerular morphological alterations were quantified by computer-assisted morphometric analysis using a method previously described (Caliari 1997). Briefly, images with 40× magnification of 30 glomeruli from each animal of different groups were randomly digitalized using a JVC TK1270/RGB microcamera (Tokyo, Japan). The KS300 software coupled to a Carl Zeiss image analyzer (Carl Zeiss, Oberkochen, Germany) was used to measure the total area (μm^2) of each glomerulus, glomerular tuft and Bowman's space. The pixels of whole glomerulus and those corresponding to the glomerular tuft were selected and used for the generation of a binary image and subsequent calculation of the corresponding areas. The area of Bowman's space was obtained by the difference between the whole glomerular area and tuft area. The regions of positive immunohistochemical reaction (expressed as μm^2) were also measured and used as a parameter to quantify venom distribution in the renal tissue.

Renal tissue proteomics

Sample preparation for mass spectrometry

The kidneys from controls and envenomed animals (at 24 h post-venom injection) were collected as described above, homogenized in cold PBS solution containing 1 % Triton X-100 with protease inhibitor cocktail (Halt protease inhibitor cocktail, Thermo, Rockford, USA) and centrifuged at 9,500×*g* for 15 min. The resulting supernatants were completely lyophilized and stored at −80 °C until use. Lyophilized samples were resuspended in water and precipitated using methanol/chloroform protocol. After precipitation, samples were dried at room temperature and resuspended in 8 M urea. Each sample containing 100 µg of protein was reduced with 5 mM tris-2-carboxyethyl-phosphine (TCEP) at room temperature for 20 min and alkylated with 10 mM iodoacetamide at room temperature in the dark for 20 min. After reduction and alkylation, proteins were digested with 2 µg of trypsin (Promega, Madison, WI) by incubation at 37 °C during 16 h. Samples were freeze-dried at −80 °C and, after thaw, formic acid to a final concentration of 5 % was added. Samples were centrifuged at 14,000 rpm for 20 min, and the supernatant was collected and stored at −80 °C.

MudPIT

The protein digest was pressure-loaded into a 250-µm i.d capillary packed with 2.5 cm of 5-µm Luna strong cation exchanger (SCX) (Whatman, Clifton, NJ) followed by 2 cm of 3-µm Aqua C18 reversed phase (RP) (Phenomenex, Ventura, CA) with a 1-µm frit. The column was washed with buffer containing 95 % water, 5 % acetonitrile and 0.1 % formic acid. After washing, a 100-µm i.d. capillary with a 5-µm pulled tip packed with 11 cm of 3-µm Aqua C18 resin (Phenomenex, Ventura, CA) was attached via a union according to Klein et al. (2012). The entire split-column was placed in line with an Agilent 1100 quaternary HPLC (Palo Alto, CA) and analyzed using a modified 11-step separation as described previously (Washburn et al. 2001). The buffer solutions used were 5 % acetonitrile, 0.1 % formic acid (buffer A), 80 % acetonitrile, 0.1 %

formic acid (buffer B), and 500 mM ammonium acetate, 5 % acetonitrile and 0.1 % formic acid (buffer C). Step 1 consisted of a 70 min gradient from 0 to 100 % (vol/vol) buffer B. Steps 2–10 had a similar profile with the following changes: 5 min in 100 % (vol/vol) buffer A, 3 min in X % (vol/vol) buffer C, a 6 min gradient from 0 to 15 % (vol/vol) buffer B and a 85 min gradient from 15 to 100 % (vol/vol) buffer B. The 3 min buffer C percentages (X) were 10, 20, 30, 40, 50, 60, 70, 80, 90 and 100 % (vol/vol), respectively, for the 10-step analysis.

LTQ-Orbitrap

As peptides eluted from the microcapillary column, they were electrosprayed directly into a LTQ-Orbitrap (Thermo Fisher) with the application of a distal 2.4-kV spray voltage. Full MS spectra were acquired in profile mode, with a mass range of 400–1,600 in the Orbitrap analyzer with resolution set at 60,000 followed by continuous repetition of 10 data-dependent MS/MS spectra at 35 % normalized collision energy was throughout each step of the multidimensional separation. Minimal signal for fragmentation was set to 1,000. Dynamic exclusion was enabled with a repeat count of 1, duration of 30.00 s, list size of 500, exclusion duration of 180.00 s and exclusion mass with high/low of 1.5 m/z. Application of mass spectrometer scan functions and HPLC solvent gradients was controlled by the Xcalibur data system.

Analysis of tandem mass spectra

MS/MS spectra were analyzed using the following software analysis protocol. Protein identification and quantification analysis were done with Integrated Proteomics Pipeline (IP2, Integrated Proteomics Applications, Inc. www.integratedproteomics.com/). Tandem mass spectra were extracted into ms2 files from raw files using RawExtract 1.9.9 (McDonald et al. 2004) and were searched using ProLuCID algorithm (Xu et al. 2006). MS/MS spectra remaining after filtering were searched with the ProLuCID algorithm against the EBI-IPI_rat_3.30_06-28-2007 concatenated to a decoy database in which the sequence for each entry in the original database was reversed (Peng et al. 2003). Searches were performed with cysteine carbamidomethylation as a fixed modification. ProLuCID results were assembled and filtered using the DTASelect program (Tabb et al. 2002) using two SEQUEST (Eng et al. 1994) defined parameters: the cross-correlation score (XCorr) and normalized difference in cross-correlation scores (DeltaCN) to achieve a false discovery rate of 1 %. The following parameters were used to filter the peptide candidates: −p 1 −y 1 –trypstat –fpf 0.01 –dm. Also, we used 50 ppm as precursor tolerance, fragment mass tolerance of 600 ppm, three as number of isotopic peaks and unlimited missed cleavages were allowed.

Assessing differential expression and exclusive proteins/bioinformatic tools

The software PatternLab (Carvalho et al. 2008, 2012) was used to identify exclusive proteins found in the control and treated conditions. PatternLab's Approximately Area Proportional Venn Diagram (AAPVD) module was used for pinpointing proteins uniquely identified in each condition. The following parameter was used: proteins that were not detected in at least 2 out of 3 runs per condition were not considered. G test spectral counting quantitation was performed in a pair-wise comparison between the two groups, as previously reported (Ambatipudi et al. 2009). Proteins are considered differentially expressed with $p < 0.1$. Ingenuity Pathway Analysis tool (Ingenuity Systems; http://www.ingenuity.com) was used to generate functional annotations of identified proteins in known molecular pathways and/or biologic function in disease. The significance of the canonical pathways and biologic function defined by identified proteins was measured in two ways: (1) The number of proteins identified from the data set that map to a known pathway or function in disease and (2) a p value (Fisher exact test) determining the probability that the association between the proteins in the data set and the canonical pathway or function in disease is explained by chance alone.

Statistical analyses

Results are expressed as mean ± SE. When appropriate, statistical comparisons were done by using one- or two-way analysis of variance followed by the Bonferroni's test. A p value of less than 0.05 was chosen to establish significance. Statistical analysis was performed using GraphPad Prism (GraphPad Software Inc., San Diego, CA, USA).

Results

Renal function

To follow renal alterations in rats, several physiological parameters were measured at different times post *Lonomia obliqua* venom injection. The results are presented in Fig. 1. Between 2 and 6 h after LOBE administration (doses of 1 mg/kg or 1.5 mg/kg, s.c.), the animals showed signs of acute toxicity, including progressive weakness, lethargy and dyspnea. Compared to PBS-treated animals, there was a reduction in body weight mainly at 6 h in rats that received the higher dose of LOBE (1.5 mg/kg, s.c.)

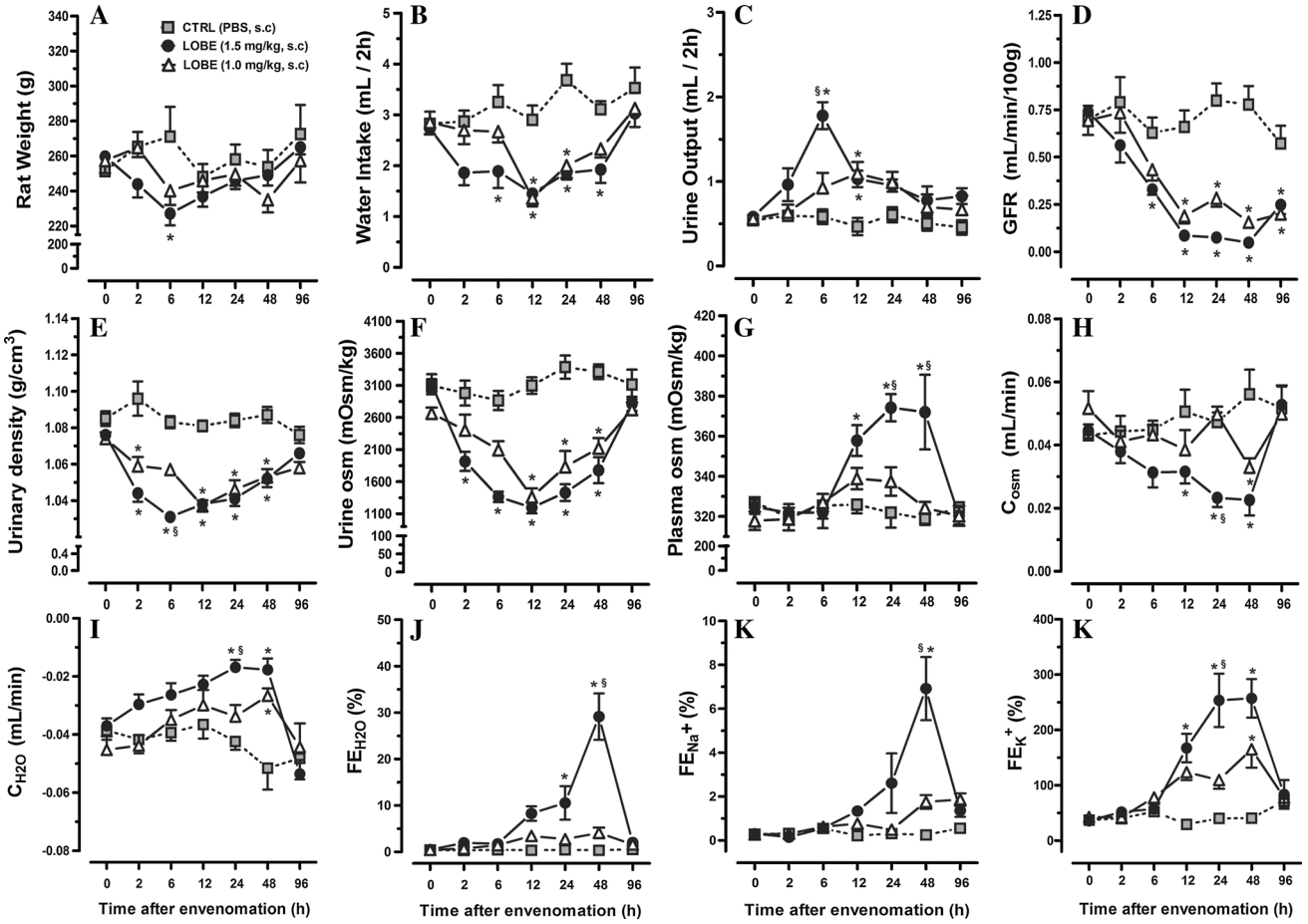

Fig. 1 Functional parameters during *L. obliqua*-induced AKI. Rats were injected subcutaneously with PBS (controls—CTRL) or LOBE (1.5 or 1.0 mg/kg). After different times post-administration, the following parameters were determined: **a** body weight, **b** water intake, **c** urine output, **d** glomerular filtration rate (GFR), **e** urinary density, **f** urine osmolality (urine osm), **g** plasma osmolality (plasma osm), **h** osmolar clearance (C_{osm}), **i** water-free clearance (C_{H2O}), **j** fractional water excretion (FE_{H2O}), **k** fractional sodium excretion (FE^{+}_{Na}) and **l** fractional potassium excretion (FE^{+}_{K}). Data are presented as mean ± SE ($n = 6$/group). Significant differences: $^{*}p < 0.05$ versus CTRL and $^{\S}p < 0.05$ versus LOBE (1.0 mg/kg, s.c)

(Fig. 1a). The weight loss was accompanied by a significant reduction in water intake between 6 and 48 h and by an increase in urinary output at 6 and 12 h for both tested doses (Fig. 1b). The polyuria was maximal at 6 h, when urinary output increased from 0.58 ± 0.08 mL/2 h in PBS-treated animals to 1.80 ± 0.16 mL/2 h ($p < 0.05$) in rats injected with LOBE (1.5 mg/kg, s.c.). At the same time, animals that received a dose of 1.0 mg/kg had a urinary output significantly lower (0.9 ± 0.2 mL/2 h, $p < 0.05$) compared to those treated with 1.5 mg/kg (Fig. 1c).

Important glomerular and tubular functions related to control of fluid filtration, water and electrolyte balance were severely impaired. Despite the polyuria, *L. obliqua*-induced AKI is associated with a marked reduction in the glomerular filtration rate (GFR). In the first 24 h of envenomation, a rapid decrease in GFR was observed in animals treated with both doses of LOBE. At 48 h, envenomed rats (injected with 1.5 mg/kg of LOBE) presented values of GFR 16 times lower than controls at the same time. This remarkable effect of the venom on GFR was observed for as long as 96 h (Fig. 1d). Similarly, the kidney's ability to concentrate urine (a primordial tubular function) was also impaired, since the density and osmolality of urine had a reduction in values between 2 and 48 h (Fig. 1e, f). The decrease in urinary osmolality was accompanied by a significant increase in the plasma osmolality observed mainly in rats injected with the higher dose of LOBE (Fig. 1g). Consistent with these results, the osmolar clearance (C_{osm}) was lower in envenomed animals, while the free water clearance (C_{H2O}) increased, which imply that the kidney is producing dilute urine through the excretion of solute-free water (Fig. 1h, i). As expected, with the loss of ability to retain water, the fractional excretion of water (FE_{H2O}) increased from 0.33 ± 0.03 % in PBS-treated animals

to 29.1 ± 4.9 % ($p < 0.05$) in rats injected with LOBE (1.5 mg/kg, s.c.) at 48 h (Fig. 1j). Likewise, tubular ability to conserve and maintain the electrolytic balance was lost throughout the envenoming period. The fractional excretion of sodium and potassium (FE_{Na+} and FE_{K+}) was high between 24 and 48 h, indicating a marked impairment in the tubular reabsorption of filtered Na^+ and K^+ (Fig. 1k, l). At 96 h, most of the renal function parameters (excepting GFR) tend to return to normal levels (similar from that obtained to non-envenomed rats).

Proteinuria

Most of envenomed animals produced dark brown-colored urine in the period of 6–12 h, indicating the occurrence of hematuria and/or hemoglobinuria. The presence of intact and fragmented erythrocytes, epithelial cells and leukocytes was observed in the urinary sediment by light microscopy (not shown). Consistent with these observations, *L. obliqua* venom-induced massive acute proteinuria, which was maximal at 6 and 12 h post-venom injection (Fig. 2a). As expected, the group treated with 1.5 mg/kg of LOBE had more severe proteinuria compared to animals treated with 1.0 mg/kg, but for both groups, urinary protein excretion decreased progressively between 12 and 48 h, reaching levels similar to controls at 96 h. Analysis of urine by SDS-PAGE revealed the presence of several proteins with molecular weights ranging from 10 to 75 kDa (Fig. 2b). A greater variety of bands were evident mainly at 6 and 12 h after envenomation, confirming this time interval as crucial to the development of glomerular injury. The two most prominent bands (observed around of 70 and 15 kDa) have molecular weights that match to serum albumin (68 kDa) and subunits of hemoglobin (16 kDa). The presence of venom excreted in urine was verified by Western blot. As shown in Fig. 2c, we detected at least 5 bands in urine from venom-treated rats at 6 and 12 h, which specifically react with antibodies raised against *L. obliqua* toxic proteins. These bands have molecular weights around of 70–60, 50, 37, 25 and 20 kDa (arrows in Fig. 2c) and were not recognized in urine from non-envenomed animals (controls). Several toxins in this range of molecular weights have already been identified through transcriptomic and proteomic analysis of LOBE. Some of them include lectins and c-type lectin-like proteins (70–60 kDa), serine proteinases (50 kDa), cysteine proteinases (37 kDa) and lipocalins (25–20 kDa) (Ricci-Silva et al. 2008; Veiga et al. 2005).

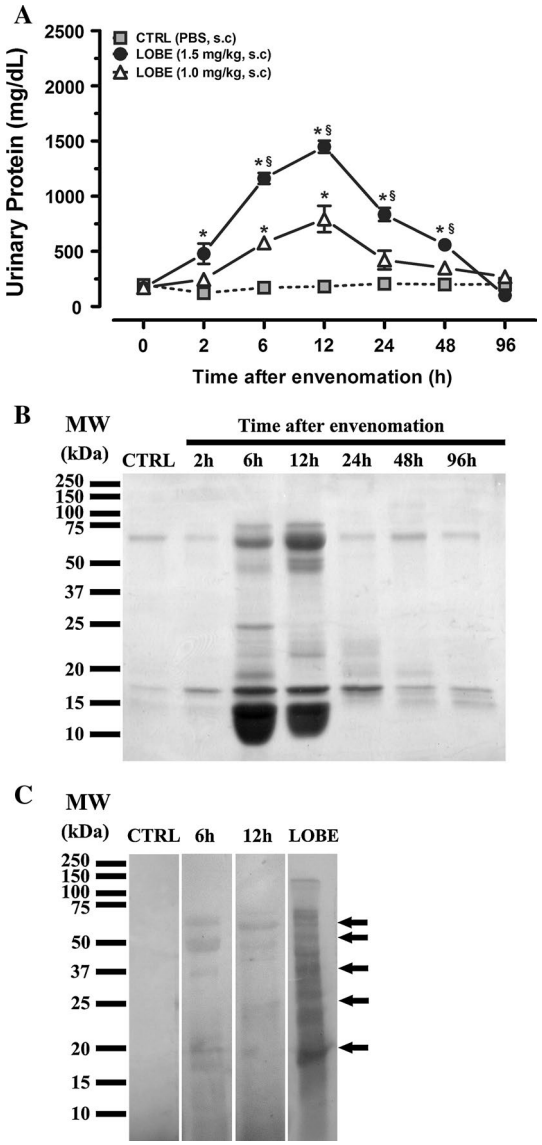

Fig. 2 Proteinuria. **a** Rats were injected subcutaneously with PBS (controls—CTRL) or LOBE (1.5 or 1.0 mg/kg). After different times post-administration, the protein levels in urine were measured. Data are presented as mean ± SE ($n = 6$/group). Statistical differences of $^*p < 0.05$ versus CTRL and $^{\S}p < 0.05$ versus LOBE (1.0 mg/kg, s.c) were considered significant. **b** Representative urine samples from CTRL and rats treated with LOBE (1.5 mg/kg, s.c.) were analyzed by SDS-PAGE (8–20 %) under reducing conditions. **c** Toxins excreted in urine were detected by Western blot. Samples of urine from CTRL and rats treated with LOBE (1.5 mg/kg, s.c.) at 6 and 12 h post-venom injection were separated by SDS-PAGE, and different toxins were detected by immunoreaction with polyclonal antibodies against LOBE. Toxins present in crude bristle extract are also showed (LOBE). The *arrows* indicate bands detected in urine samples at 6 and 12 h of envenomation. Molecular weight (MW) standards were shown on the left of figure **b** and **c**

Renal histopathological alterations

Light microscopy of kidney biopsies from PBS-injected rats revealed a normal renal parenchyma (Fig. 3a). In contrast, envenomed animals showed progressive degenerative lesions compatible with acute tubular necrosis (ATN) (Fig. 3b–h). Increased acidophilia and dilation of renal tubules were observed between 6 and 48 h after venom

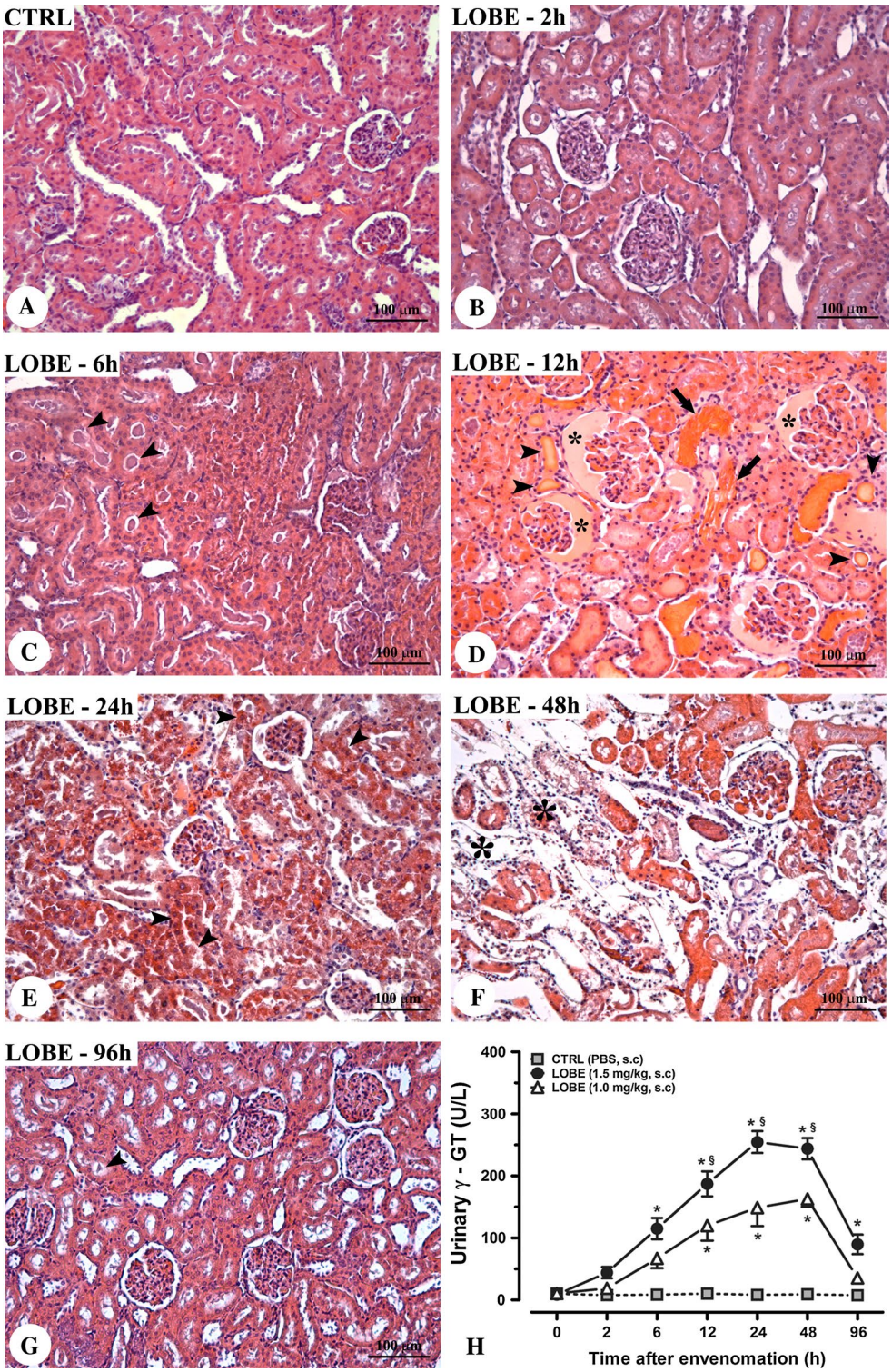

Fig. 3 *L. obliqua* envenomation induces acute tubular necrosis. Representative kidney sections from control (CTRL) or envenomed animals (injected with 1.5 mg/kg, s.c.) are presented (**a**–**g**). Note the normal morphology of kidney from CTRL animal (**a**) in comparison with the progressive degenerative lesions of venom-treated rats (**b**–**g**). Increased acidophilia, dilation of renal tubules, loss of proximal brush border, cytoplasm vacuolation, nuclear pyknosis and desquamation of necrotic cells can be observed (**d**–**f**). Hyaline (*arrowheads* in **c**, **d** and **g**) and hematic (*arrows* in **d**) casts are also present inside renal tubules. *Arrowheads* in E indicate necrotic cells. *Asterisks* in **d** and **f** indicate the presence of a hyaline material within the Bowman's space and an inflammatory cell infiltrate and edema, respectively. All sections were stained with H&E. Magnification: ×10. **h** Levels of urinary γ-glutamyl transferase (γ-GT) activity were measured in rats injected with PBS or LOBE (1.5 or 1.0 mg/kg) at different times post-administration. Data are presented as mean ± SE ($n = 6$/group). Statistical differences of $^{*}p < 0.05$ versus CTRL and $^{\S}p < 0.05$ versus LOBE (1.0 mg/kg, s.c) were considered significant

administration (Fig. 3c–f). Loss of proximal brush border, cytoplasm vacuolation, and in some tubules, degeneration and desquamation of necrotic cells occurred between 12 and 48 h (Fig. 3d–f). The nuclei of the various proximal tubular cells at 24 and 48 h often showed pyknosis with clumping of chromatin material (Fig. 3e, f). In several tubules at 48 h, the renal epithelium was completely necrotic, whereas the basement membrane was either intact or disrupted by tubular necrosis (Fig. 3f). Consistent with the histological signs of tubular injury, γ-GT urinary activity—which is considered an efficient biomarker for early diagnosis of ATN (Guder and Ross 1984)—increased in a

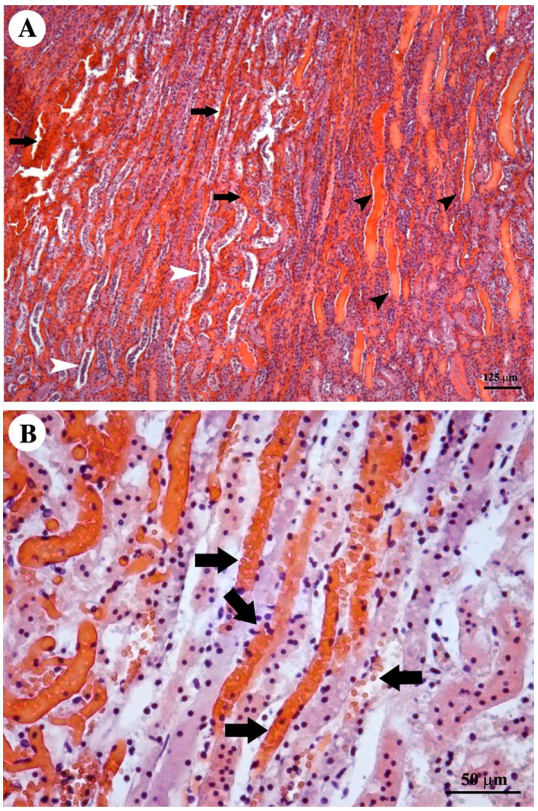

Fig. 4 *L. obliqua* envenomation induces renal tubular obstruction. Representative kidney sections from animals injected with LOBE (1.5 mg/kg, s.c.) showing details of tubular obstruction by hyaline and hematic casts and cellular debris at 12 h (**a**) and 24 h (**b**) post-venom injection. Hyaline casts (*black arrowheads*) are formed by a protein-rich material (predominantly serum albumin and hemoglobin), while hematic casts (*black arrows*) are formed by fragmented or intact erythrocytes. Due to tubular necrosis, the basement membrane in some tubules is disrupted, resulting in detachment of necrotic cells into the lumen (*white arrowheads*). All sections were stained with H&E. Magnification: ×4 (**a**) and ×20 (**b**)

dose- and time-dependent manner up to 48 h. At 96 h, γ-GT activity decreased, but remained significantly high in animals treated with 1.5 mg/kg of LOBE. Histologically, the signs of lesions were much less marked, and the proximal and post-proximal tubular epithelia assumed a normal appearance at 96 h (Fig. 3g, h).

Besides the evidence of degenerative lesions, proximal and distal tubules also had swollen lumens. Hyaline and hematic casts and cellular debris were found within tubules, obstructing their lumens (Figs. 3c–f, 4). Hyaline casts (predominantly formed by a protein-rich material) were more prevalent at 6 and 12 h (Figs. 3c, d, 4a), while hematic casts (predominantly formed by fragmented or intact erythrocytes) and cellular debris have appeared commonly at 12, 24 and 48 h (Figs. 3d–f, 4a, b).

An intense inflammatory response characterized by edema, cellular infiltration and fibrosis was observed mainly at 48 and 96 h (Figs. 3f, 5). Inflammatory cell infiltrate and edema were detected at 48 h in regions of extensive necrosis (Fig. 3f) and within glomeruli (Fig. 5c). At 96 h, despite signs of tubular regeneration, the inflammatory infiltrate increased significantly, probably to help in tissue repair (Fig. 5b). Light microscopy of sections stained with picrosirius revealed extensive peritubular collagen deposition at 96 h after administration of *L. obliqua* venom (Fig. 5e) compared to PBS-treated rats (Fig. 5d), indicating fibrosis. Foci of inter-glomerular collagen deposition were also observed in the renal cortex at the same time (Fig. 5f).

Glomerular morphometric alterations and renal tissue factor activity

Glomerular alterations in envenomed animals were associated with lobulation of the capillary tufts, dilation of glomeruli, deposition of a hyaline material inside the Bowman's space and distention of Bowman's space (Figs. 3d, 6a, 7b). Nodules that formed a dense, strongly stained mesangial matrix evidenced by the presence of a PAS-positive stain in the capillary tufts were also observed between 2 and 12 h post-venom (Fig. 6a). Consistent with histological observations, computer-assisted morphometric analysis has indicated a significant increase in glomerular area at all-time intervals examined. There was also an increase in the areas of glomerular tuft and Bowman's space, which confirms that the capillaries and Bowman's space are dilated (Fig. 6b). The enlargement of Bowman's space observed at 12 h possibly is related to the presence of a hyaline material (rich in plasma proteins) found in several glomeruli at this time (details in Figs. 3d, 7b).

Since intra-glomerular fibrin deposition can impair renal function and *L. obliqua* venom is able to activate the coagulation system both in vitro and in vivo (Berger et al. 2010), we decide to measure the levels of renal tissue factor (TF) activity during envenomation. TF is a transmembrane enzyme activator that triggers the coagulation cascade, generating activated factor X and fibrin. As showed in Fig. 6c, renal TF activity increased rapidly from the first 2 h, reaching levels twice higher than control values at 6 h. At 12 and 24 h post-venom injection, this level remained significantly high, but decreased progressively thereafter (Fig. 6c). Interestingly, the rise in renal TF activity was coincident with the presence of PAS-positive deposits (which stain specifically glycoproteins) within the capillary tufts at 2–12 h (Fig. 6a).

Hemodynamics and renal vascular permeability

Mean arterial blood pressure was lower in animals that received LOBE compared to basal levels in controls (Table 1). Sustained hypotension was detected between

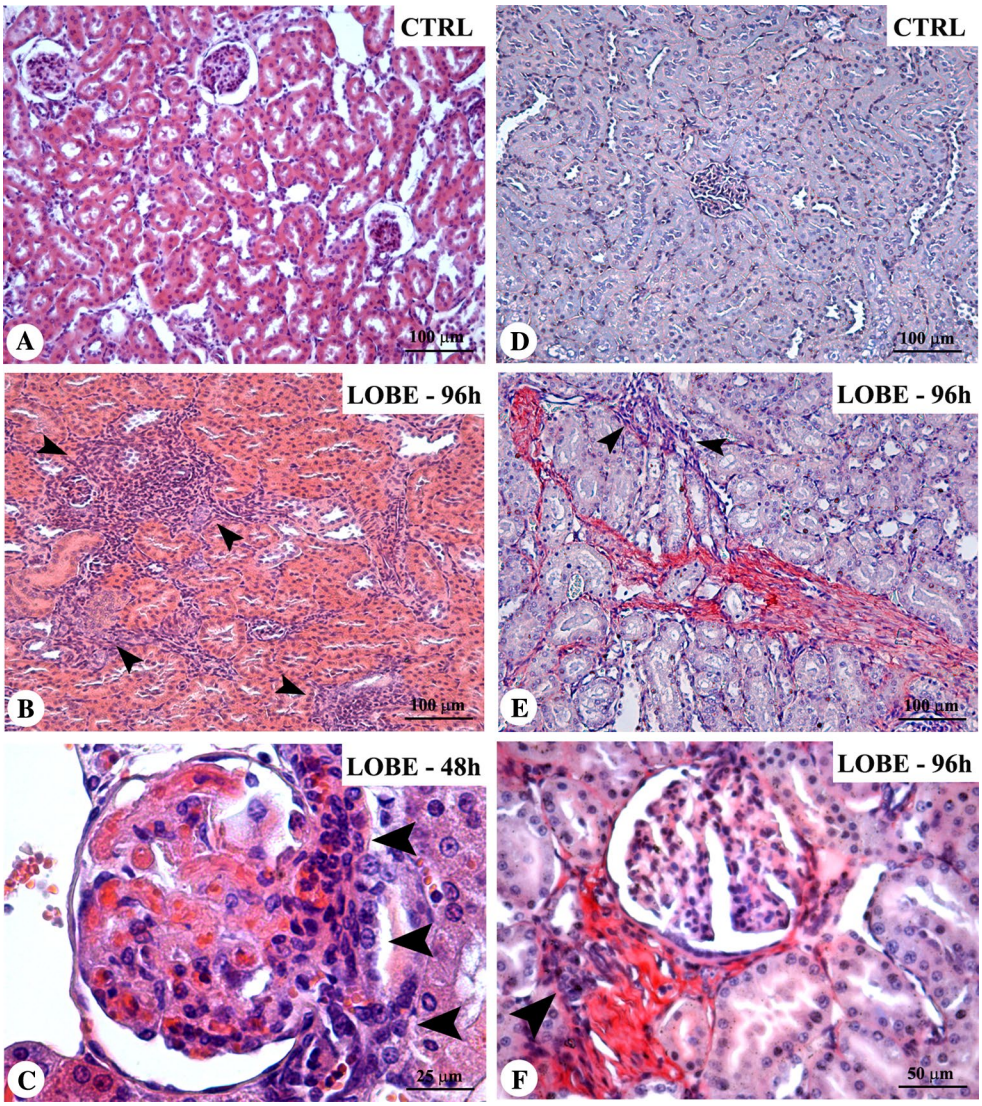

Fig. 5 *L. obliqua* envenomation induces renal inflammation and fibrosis. Light micrographs showing a marked inflammatory cell infiltrate (*arrowheads*) in the tubulointerstitial region at 96 h (**b**) and glomerulus at 48 h (**c**) after LOBE injection (1.5 mg/kg, s.c.). There were no signs of inflammation in control (CTRL) animals (**a**). It was also observed an extensive peritubular (**e**) and inter-glomerular (**f**) collagen deposition at 96 h (regions stained in red), indicating fibrosis. *Arrowheads* in these panels indicate inflammatory infiltrate. There were no signs of fibrosis in CTRL rats (**d**). Stain: H&E (**a**–**c**) and picrosirius (**d**–**f**). Magnification: ×10 (**a**, **b**, **d** and **e**), ×20 (**f**) and ×40 (**c**)

24 and 96 h in rats treated with the both doses of venom. The maximum decrease occurred at 24 h. In contrast, the heart rate increased significantly at 12 and 96 h in animals injected with 1 mg/kg of LOBE and at 48 h in animals injected with 1.5 mg/kg. Hypotension was accompanied by an increase in renal vascular permeability (Fig. 7). Kidney blood vessels were hyperemic, and signs of plasma leakage, migration of inflammatory cells and interstitial edema were also evident after 12 h of venom administration (Fig. 7a). As mentioned above, several glomeruli at 12 h have their Bowman's space filled with a protein-rich material that had extravasated from glomerular capillaries (Fig. 7b). Confirming these observations, a marked increase in vascular permeability in the kidney, as measured by the extravasation of Evans blue dye, was detected at 12 and 24 h after LOBE injection (1.5 mg/kg, s.c) (Fig. 7c).

Immunohistochemical detection of venom in the renal tissue

Venom distribution and its binding to renal structures was investigated by submitting kidney biopsies from venom-treated and control rats to immunohistochemistry using anti-LOBE IgG that reacts specifically with venom toxins

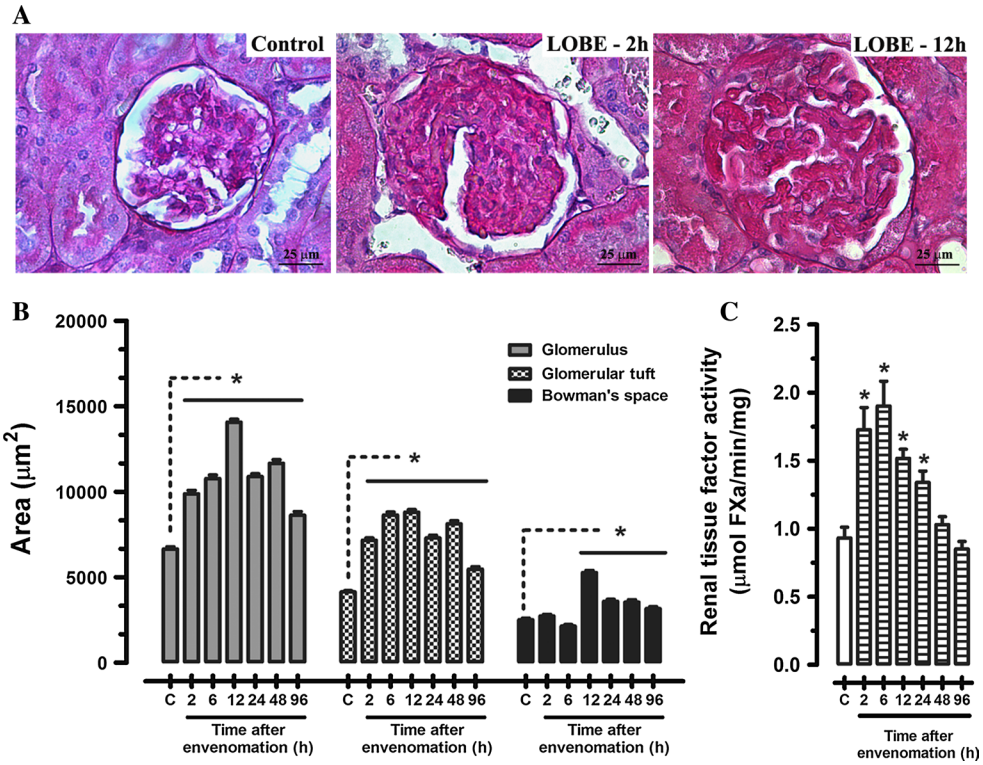

Fig. 6 Glomerular alterations. **a** Light micrographs showing a time-dependent increase in the deposition of a PAS-positive material in glomerular capillaries of LOBE-injected animals (1.5 mg/kg, s.c.) in comparison with controls. Also note the increase in glomerular size. All sections were stained with PAS. Magnification: ×40. **b** Thirty glomeruli from each animal injected with the dose of 1.5 mg/kg were used to quantify the mean area of glomerulus, glomerular tuft and Bowman's space of animals treated with the dose of 1.5 mg/kg. Data are presented as mean ± SE ($n = 6$/group). Statistical differences of $^*p < 0.05$ in comparison with the respective control (C) were considered significant. **c** Renal tissue factor activity was measured in control (C) and envenomed (1.5 mg/kg, s.c.) animals by generation of factor Xa (FXa). Data are presented as mean ± SE ($n = 6$/group). Statistical differences of $^*p < 0.05$ were considered significant in comparison with the respective control

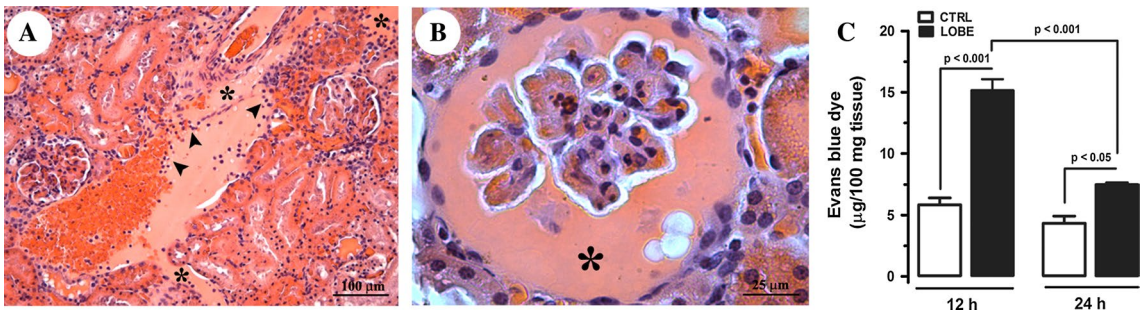

Fig. 7 Renal vascular permeability. Representative micrographs of a kidney blood vessel (**a**) and glomerulus (**b**) from animals injected with LOBE (1.5 mg/kg, s.c.) after 12 h of envenomation. Note the vascular leakage and edema (*asterisks*) and migration of inflammatory cells to damaged tissue (*arrowheads*). Also, the presence of a hyaline material inside the Bowman's space (*asterisk* in **b**) was associated with the increase in glomerular area observed at this time. All sections were stained with H&E. Magnification: ×10 (**a**) and ×40 (**b**). **c** Evaluation of changes in renal vascular permeability were assessed by Evans blue dye extravasation. Results are expressed as µg Evans blue dye per 100 mg of renal tissue from control (CTRL) and LOBE-treated (1.5 mg/kg, s.c.) rats at 12 and 24 h post-venom administration. Data are presented as mean ± SE ($n = 6$/group). Statistical comparisons are indicated

(Fig. 8). Positive immunohistochemical reaction was found in cortical and medullar regions of kidneys from rats injected with 1.5 mg/kg of LOBE (Fig. 8d, c). Venom was detected in glomerular capillaries, Bowman's capsule, in proximal and distal tubules and in intra-tubular casts. Staining for venom was intense in tubular brush border at 2 and

Table 1 Hemodynamic parameters

Parameter	Group	Time after envenomation (h)						
		0	2	6	12	24	48	96
MAP (mmHg)	CTRL	94.6 ± 2.2	107.5 ± 1.5	100.2 ± 3.4	96.3 ± 1.2	115 ± 12.2	111.4 ± 1.1	118 ± 12.6
	LOBE (1.0 mg/kg, s.c.)	103 ± 3.8	92.8 ± 2.6	104.3 ± 2.7	84.5 ± 3.6	88 ± 3.1*	91.6 ± 1.5*	91.7 ± 3.5*
	LOBE (1.5 mg/kg, s.c.)	104 ± 2.3	124.8 ± 8.6§	112.7 ± 4.8	95.1 ± 2.9	74.9 ± 1.5*,§	81.5 ± 1.1*	95.1 ± 1.4*
HR (Beats/min)	CTRL	366 ± 5.4	391 ± 1.8	391 ± 5.8	403 ± 2.1	401 ± 4.1	362 ± 11.3	376 ± 8.7
	LOBE (1.0 mg/kg, s.c.)	383 ± 3.7	402 ± 16.1	409 ± 13.1	449 ± 6.9*	398 ± 11.4	381 ± 8.5	443 ± 8.5*
	LOBE (1.5 mg/kg, s.c.)	355 ± 7.2	390 ± 14.3	391 ± 5.4	393 ± 10.2§	427 ± 6.6§	424 ± 5.7*,§	369 ± 3.3§

Data are presented as mean ± SE ($n = 6$/group)

MAP mean arterial pressure, *HR* heart rate

Statistical differences of * $p < 0.05$ versus CTRL and § $p < 0.05$ versus LOBE (1.0 mg/kg, s.c) were considered significant

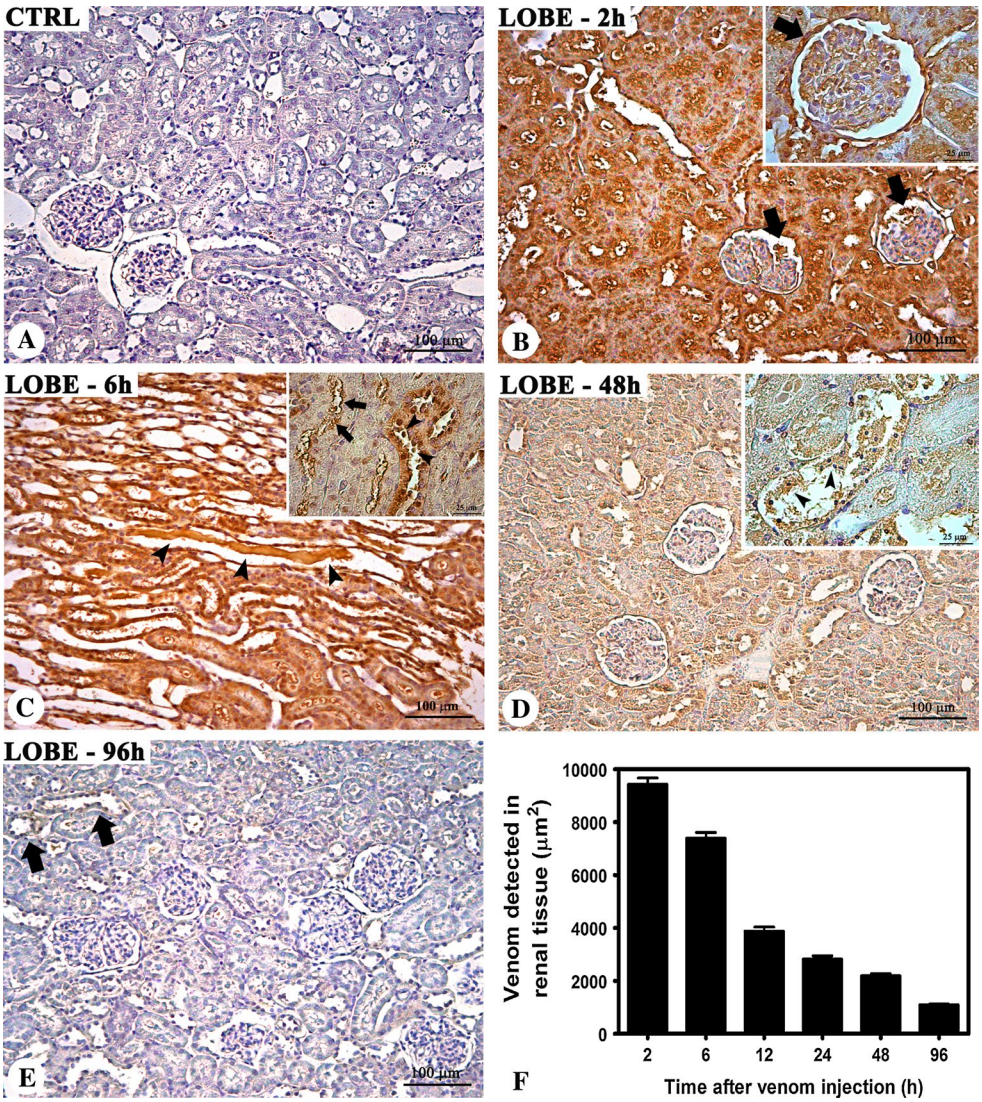

Fig. 8 Immunohistochemical detection of *L. obliqua* venom in renal tissue. Positive immunohistochemical reaction was found in cortical and medullar regions of kidneys from rats injected with 1.5 mg/kg of LOBE (**b**–**e**). Venom was detected in glomerular capillaries (*arrows* in **b**), Bowman's capsule (*arrow* in the inset B), tubular brush border (*arrows* in the inset C), in intra-tubular casts (*arrowheads* in **c**) and also was present in cells of tubules in degeneration (*arrowheads* in the insets **c** and **d**). After 96 h, the immunoreactivity for venom was weak and mainly localized in tubules (*arrows* in **e**). There was no immunoreactivity in the renal structures of control (CTRL) rats (**a**). Magnification: ×10 (**a**–**e**) and ×40 (*insets* in **b**–**d**) **f**. The amounts of venom detected in renal tissue were estimated by the area of positive immunohistochemical reaction. Thirty sections per rat were analyzed as described in "Materials and methods." Data are presented as mean ± SE ($n = 6$/group)

6 h and was also present in cells of tubules in degeneration at 48 h (Fig. 8b–d). Generally, tubules stained more than glomeruli. There was no immunoreactivity for venom in the renal structures of PBS-treated rats (controls) (Fig. 8a). The highest levels of venom (estimated by the area of positive immunohistochemical reaction) were detected in the

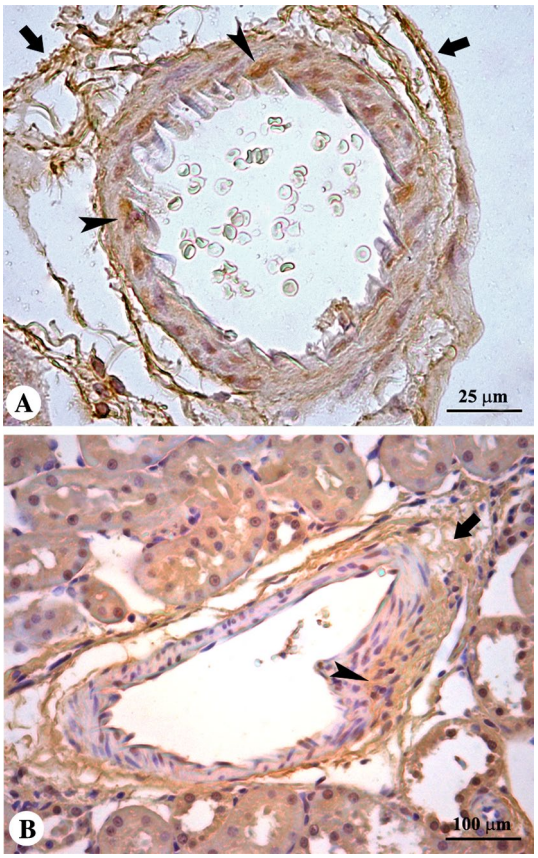

Fig. 9 Immunohistochemical detection of *L. obliqua* venom in renal vascular tissue. Positive immunohistochemical reaction was detected in renal arteries (**a**) and veins (**b**) of rats injected with LOBE (1.5 mg/kg, s.c.) at 6 h of envenomation. Note the presence of venom in perivascular connective tissue (*arrows*) and endothelium and smooth muscle cells (*arrowheads*). Magnification: ×10 (**b**) and ×40 (**a**)

renal tissue at 2 h (Fig. 8f). After that, venom immunoreactivity decreased progressively until 96 h when the staining was weak (Fig. 8e, f). *L. obliqua* toxins were also detected in other kidney structures such as in perivascular connective tissue of blood vessels, endothelium and smooth muscle of arteries and veins (Fig. 9a, b).

Kidney proteins differentially expressed during envenomation

To gain further mechanistic insight which drive venom-induced kidney disease, we applied a semi-quantitative discovery-based shotgun proteomic approach to identify the proteins differentially expressed in the kidney of envenomed animals. For this purpose, the proteomic data were acquired by tandem mass spectrometry with subsequent quantification, analysis of differential protein expression, validation and functional annotations in order to identify the involved molecular pathways. The proteins identified consist of two classes: (1) those that were differentially expressed and met our significance criteria and (2) proteins that were uniquely identified in kidneys of rats injected with PBS or LOBE (1.5 mg/kg) after 24 h. Figure 10a represents differentially expressed and unique proteins via a Venn diagram. Overlaps between PBS- and LOBE-treated animals represent significant differentially expressed proteins, and non-overlapping portions of the diagram represent unique protein identifications. A total of 779 proteins were identified. Twenty-four proteins were exclusively identified in envenomed animals; 169 were exclusively identified in control rats, and 586 were common proteins in both treatments. Among these 586 proteins, 138 (23.5 %) were identified as being differentially expressed.

Ingenuity pathway analysis was used for functional annotations and revealed several key protein categories and pathways significantly enriched in the differentially expressed proteins. Thus, the sets of proteins were assigned to either biologic function in disease or canonical signaling pathways. Through these analyses, it was evident that the set of proteins identified in control kidneys displayed healthy biological functions such amino acid metabolism and small-molecule biochemistry associated with normal renal metabolic pathways (Fig. 10b). On the other hand, protein expression shifts toward "cellular distress" functions in the kidney of envenomed rats (Fig. 10c). In this case, the expression profiles were considerably enriched for proteins that belong to acute-phase inflammatory response signaling, LXR/RXR activation (involved in retinoic acid-mediated gene activation triggered by inflammatory stimulus), oxidative stress response pathways such as that mediated by the nuclear erythroid-related factor 2 (NRF2) and coagulation and complement systems (involved in thrombosis, fibrosis, inflammation and vascular alterations) (Fig. 10c).

Accordingly to our functional and histopathological results, several novel proteins related to renal disease were identified in the kidney of LOBE-treated animals. Proteins associated with tubular and glomerular injury, necrosis, inflammation and fibrosis were up-regulated or unique in envenomed rats (Fig. 10d). Some of these molecules, mainly those that were related to renal disease or identified in canonical pathways, are listed in Table 2. A complete list with differentially expressed and unique proteins of envenomed and control animals are shown in supplemental Table 1. It is worth mentioning that proteins functionally linked to tissue injury (markers of necrosis and/or apoptosis), osmotic and oxidative stress, electrolytic imbalance, acute-phase inflammatory response, fibrosis and thrombosis were expressed in the kidneys of LOBE-treated rats (Table 2). Proteins of the kallikrein-kinin and complement systems which are related to hypotension and control of vascular permeability were also found to be up-regulated in envenomed animals (Table 2). Our proteomic data also

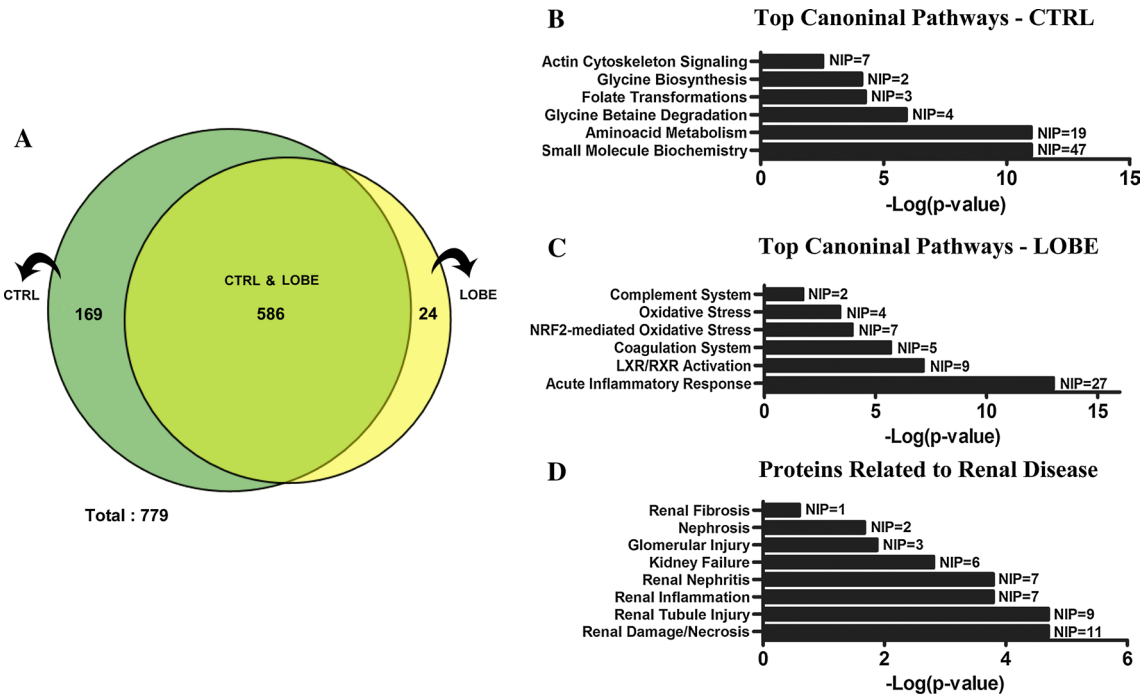

Fig. 10 Kidney proteins differentially expressed during *L. obliqua* envenomation. Unique or differentially expressed kidney proteins from control and envenomed (1.5 mg/kg, s.c.) animals were identified at 24 h post-venom injection by proteomic analysis. Exclusive and common proteins in each condition, as well as the total number of proteins identified are showed via a Venn diagram (**a**). Top canonical pathways of differentially expressed and unique proteins identified in control (CTRL) (**b**) and LOBE-treated (**c**) kidneys are shown. Those proteins functionally related to renal disease were also categorized accordingly to their roles in different types of renal pathologies (**d**). Each functional annotation is assigned to a significance score represented as *p* value (Fisher exact test) determining the probability that the association between the proteins in the data set and the canonical pathway or function in disease is explained by chance alone. The number of identified proteins (NIP) that belong to a particular canonical pathway or play a role in renal pathology is shown

confirm that an important mechanism of *Lonomia*-induced AKI is mediated by hemoglobin and the release of its degradation products: free heme and iron. In fact, hemoglobin, hemopexin and ferritin were up-regulated, and the expression of heme oxygenase-1 was uniquely induced in the kidneys of envenomed rats (Table 2). As a result of heme and iron release, several antioxidant enzymes were found to be up-regulated, indicating the generation of reactive oxygen species (Table 2).

Discussion

AKI is frequently described and is life threatening in several cases of snake and arthropod envenomation (Sitprija 2006; Berger et al. 2012). Particularly in *Lonomia obliqua* envenomation, AKI is the main cause of death and its mechanisms are completely unknown until now. In this work, we use an in vivo experimental model to characterize the *L. obliqua*-induced AKI. According to our results, the pathophysiological mechanism seems to be complex and multifactorial involving four main issues: (1) vascular abnormalities; (2) tubular and glomerular alterations; (3) renal inflammation and (4) a direct venom cytotoxic activity.

Vascular abnormalities

Rats injected with *L. obliqua* venom presented important hemodynamic alterations characterized by systemic hypotension and increased heart rate. The time of maximal decrease in blood pressure was coincident with the reduction in GFR and the impairment of renal function. In addition, an increase in renal vascular permeability and edema was also observed at the same period of envenomation. These findings are important because systemic vasodilation is associated with the decrease in GFR and can lead to renal hypoperfusion and ischemia in different pathological conditions (Schrier et al. 2004). Specifically in this type of envenomation, one mechanism that could contribute to vasodilation is the activation of kallikrein-kinin system (KKS). It is known that *L. obliqua* venom has toxins (kallikrein activators and kininogenases) able to activate plasma prekallikrein and directly release bradykinin (BK) from low molecular weight kininogen (LMWK) (Pinto et al. 2010; Bohrer et al. 2007). Interestingly, our results indicated

Table 2 Unique and differentially expressed proteins identified in the kidneys of rats envenomed by *L. obliqua*

Acession number[a]	Protein description	Fold change[b]	*p* value[c]	Biological function and/or participation in disease	References
Up-regulated					
P24090	Alpha-2-HS-glycoprotein	6.034	0.004	Cysteine-type endopeptidase inhibitor activity/acute-phase response/regulation of inflammatory response/up-regulation of Ahsg2 is associated with inflammation and tissue edema	Bowler et al. (2004)
P02764	Alpha-1-acid glycoprotein (Orm1)	5.093	0.001	Acute-phase inflammatory response to antigenic stimulus/up-regulated in response to LPS/Orm1 is considered an early and accurate biomarker of AKI	Devarajan et al. (2010)
P11517	Hemoglobin subunit beta-2 (HbB)	4.395	0.001	Oxygen transport/up-regulation of Hb is nephrotoxic and associated with kidney injury in several diseases including sepsis, type 2 diabetes and *Crotalus* envenomation	Zager (1996), Pinho et al. (2005), Larsen et al. (2010)
Q76MJ6	YBX1	3.37	0.04	DNA-binding/upregulation of Ybx1 mRNA in kidney is associated with proximal tubular injury in male rat	Thukral et al. (2005)
Q6LE95	Low molecular weight kininogen (LMWK)	3.282	0.001	Acute-phase inflammatory response/precursor of the active peptide bradykinin (BK)/related to vasodilation, hypotension and increase in vascular permeability/participates of the contact-phase reactions of blood coagulation and kallikrein-kinin system/*L. obliqua* venom is able to release BK from LMWK	Bohrer et al. (2007), Pinto et al. (2010)
Q921A4	Cytoglobin (Cygb)	3.003	0.015	Heme and iron binding/up-regulated in conditions of oxidative stress/plays a role in the development of renal fibrosis/overexpression of Cygb improved histological renal injury, preserved renal function and ameliorated fibrosis	Mimura et al. (2010), Nishi et al. (2011)
Q9R063	Peroxiredoxin-5, mitochondrial (Prdx-5)	2.796	0.001	Involved in redox regulation of the cell/eliminating peroxides generated during metabolism/play a major role in the cellular response to oxidative stress/up-regulated in conditions of renal ischemia–reperfusion injury and hypoxia	Godoy et al. (2011)
P70388	DNA repair protein (Rad50)	2.713	0.061	DNA repair/plays a central role in double-strand break repair/up-regulation of Rad50 mRNA is associated with hepatocellular carcinoma	Stefanska et al. (2011)
P02793	Ferritin light chain 1	2.563	0.001	Ferric iron binding/iron homeostasis and metabolism	Zager (1996), Zager et al. (2012)
P08932	T-kininogen 2 (isoform 2 of LMWK)	2.128	0.001	Acute-phase inflammatory response/precursor of the active peptide bradykinin (BK)/related to vasodilation, hypotension and increase in vascular permeability/participates in the contact-phase reactions of blood coagulation and kallikrein-kinin system/*L. obliqua* venom is able to release BK from LMWK	Bohrer et al. (2007), Pinto et al. (2010)
P02770	Serum Albumin (Alb)	2.096	0.018	The main protein of plasma/involved in molecular transport/regulation of the colloidal osmotic pressure of blood/up-regulation of serum albumin mRNA and albuminuria is associated with proximal tubular and glomerular injury and interstitial nephritis in male rat	Thukral et al. (2005)
P09006	Serine protease inhibitor A3 N	1.891	0.001	Acute-phase inflammatory response/induced by IL-1, IL-6 and interferon-γ/up-regulated during sepsis	Chinnaiyan et al. (2001)
P31977	Ezrin	1.706	0.032	Involved in connections of major cytoskeletal structures to the plasma membrane of glomerular epithelium cells (podocytes)	Thukral et al. (2005), Trof et al. (2006)

Table 2 continued

Acession number[a]	Protein description	Fold change[b]	*p* value[c]	Biological function and/or participation in disease	References
P35704	Peroxiredoxin-2 (Prdx-2)	1.691	0.015	Involved in redox regulation of the cell/eliminating peroxides generated during metabolism/play a major role in the cellular response to oxidative stress/up-regulated in conditions of renal ischemia–reperfusion injury and hypoxia	Godoy et al. (2011)
Q6P9V2	Ferritin, heavy polypeptide 1	1.543	0.012	Stores iron/important for iron homeostasis	Zager (1996), Zager et al. (2012)
P14942	Glutathione S-transferase alpha-4 (GST)	1.516	0.032	Antioxidant enzyme/conjugation of reduced glutathione to a wide number of exogenous and endogenous hydrophobic electrophiles/it is a marker of proximal tubular injury	Thukral et al. (2005), Trof et al. (2006)
P01946	Hemoglobin subunit alpha-1/2 (HbA)	1.495	0.001	Oxygen transport/up-regulation of Hb is nephrotoxic and associated with kidney injury in several diseases including sepsis, type 2 diabetes and *Crotalus* envenomation	Larsen et al. (2010), Pinho et al. (2005), Zager (1996)
B1H216	Hemoglobin alpha, adult chain 2 (HbB)	1.495	0.001	Oxygen transport/up-regulation of Hb is nephrotoxic and associated with kidney injury in several diseases including sepsis, type 2 diabetes and *Crotalus* envenomation	Larsen et al. (2010), Pinho et al. (2005), Zager (1996)
P07335	Creatine kinase B-type (CK-B)	1.452	0.012	Creatine kinase isoenzymes play a central role in energy transduction in tissues. In the kidney, localized primarily in the outer medulla in the thick ascending limb and distal convoluted tubule/marker of acute tubular injury	Shashidharamurthy et al. (2010)
P01026	Complement C3 (Neutrophil chemotactic factor-1)	1.319	0.044	Plays a central role in the activation of the complement system/its processing by C3 convertase is the central reaction in both classical and alternative complement pathways/it is a mediator of local inflammatory process/it induces the contraction of smooth muscle/increases vascular permeability/causes histamine release from mast cells and basophilic leukocytes/acts as a chemoattractant for neutrophils/complement activation increases tubulointerstitial fibrosis of the kidney	Turnberg et al. (2006)
P07483	Fatty Acid Binding Protein 3 (FABP3)	1.286	0.001	FABP3 are thought to play a role in the intracellular transport of long-chain fatty acids and their acyl-CoA esters/upregulation of FABP3 mRNA in kidney is associated with proximal tubular injury in male rat	Thukral et al. (2005)
Q9JJ19	Na^+/H^+ exchange regulatory cofactor NHE-RF1	1.196	0.053	Sodium transporter localized in apical membrane of proximal tubular cells/important in renal sodium transport and phosphate absorption/it is a marker of tubular injury	Trof et al. (2006)
P17475	Serpin 1 Alpha-1-antiproteinase	1.175	0.071	Acute-phase inflammatory response/response to hypoxia/inhibitor of serine proteases/has affinity for plasmin and thrombin/Serpine1 is involved in damage of tubulointerstitium and is up-regulated in case of disseminated intravascular coagulation (DIC)	Eddy (2004)
P32038	Complement factor D (C3 convertase activator)	1.144	0.017	Plays a central role in the activation of the complement system/factor D cleaves factor B when the latter is complexed with factor C3b, activating the C3bbb complex, which then becomes the C3 convertase of the alternate pathway. Its function is homologous to that of C1s in the classical pathway/complement activation increases tubulointerstitial fibrosis in the kidney	Turnberg et al. (2006)

Table 2 continued

Acession number[a]	Protein description	Fold change[b]	*p* value[c]	Biological function and/or participation in disease	References
P04276	Vitamin D-binding protein (DBP)	1.088	0.011	It carries the vitamin D sterols and prevents polymerization of actin by binding its monomers. DBP associates with membrane-bound immunoglobulin on the surface of B lymphocytes and with IgG Fc receptor on the membranes of T lymphocytes/DBP knockout mice displayed decreased damage in renal cortex	Safadi et al. (1999)
O88767	Protein DJ-1	1.07	0.001	Protects cells against oxidative stress and cell death/eliminates hydrogen peroxide/may act as an atypical peroxiredoxinlike peroxidase that scavenges hydrogen peroxide	Godoy et al. (2011)
P04041	Glutathione peroxidase 1	1.059	0.096	Antioxidant enzyme/protects the hemoglobin in erythrocytes from oxidative breakdown	Zager (1996), Basnakian et al. (2002), Khan (2009)
P62898	Cytochrome c, somatic (CytC)	1.003	0.004	Electron carrier protein/plays a role in apoptosis/suppression of the anti-apoptotic members or activation of the proapoptotic members of the Bcl-2 family leads to altered mitochondrial membrane permeability resulting in release of cytochrome c into the cytosol/increases apoptosis in kidney tubule epithelial cells	Chang et al. (2000)
P20059	Hemopexin (Hpx)	0.951	0.065	Participate in heme metabolism/binds and neutralizes pro-oxidant free heme/potentially impacts heme–iron-mediated tubular injury	Zager et al. (2012)
P07632	Superoxide dismutase [cu–zn] (SOD)	0.606	0.001	Antioxidant enzyme/destroys radicals which are normally produced within the cells and which are toxic to biological systems	Zager (1996), Basnakian et al. (2002), Khan (2009)
Down-regulated					
Q63213	Alpha-2u globulin	5.33	0.001	Associated with proximal tubule necrosis and protein droplet accumulation in male rats/it is down-regulated in chronic hypoxia in the kidney	Son et al. (2008)
P97615	Thioredoxin, mitochondrial	4.301	0.008	Has an anti-apoptotic function/plays an important role in the regulation of mitochondrial membrane potential/response to hypoxia/response to oxidative stress	Godoy et al. (2011)
Q03626	Murinoglobulin-1	3.268	0.045	Peptidase inhibitor activity/acute-phase inflammatory response/it is down-regulated by up to 70 % during acute inflammation or tumor development	Thukral et al. (2005)
Q64565	Alanine–glyoxylate aminotransferase 2, mitochondrial	3.112	0.08	Enzyme responsible by the metabolism of dimethylarginine (ADMA)/ADMA is a potent inhibitor of nitric oxide (NO) synthase/this activity provides mechanism through which the kidney regulates blood pressure/its inhibition decreases the production of NO	Caplin et al. (2012)
D3ZKG1	Methylmalonyl-CoA mutase, mitochondrial (Mut)	2.55	0.05	Involved in the degradation of several amino acids, odd-chain fatty acids and cholesterol via propionyl-CoA to the tricarboxylic acid cycle/knockout mouse for Mut gene displayed increased tubulointerstitial nephritis	Chandler et al. (2009)
Q62980	Heparin sulfate proteoglycan 2 (HSPG2)	2.391	0.001	Cell adhesion protein/increase glomerular and mesangial kidney proliferation/positive regulation of endothelial cell proliferation/response to hypoxia	Chen et al. (2001)
P11232	Thioredoxin	2.191	0.009	Participates in various redox reactions through the reversible oxidation of its active center/cell redox homeostasis	Godoy et al. (2011)

Table 2 continued

Acession number[a]	Protein description	Fold change[b]	*p* value[c]	Biological function and/or participation in disease	References
Q920P6	Adenosine deaminase	2.139	0.019	Catalyzes the hydrolytic deamination of adenosine/its inhibition leads to accumulation of adenosine, which has a potent afferent arteriolar vasodilator effect through A_{2B} receptors located in glomerular vessels/adenosine also has a platelet aggregation inhibitory activity	Feng and Navar (2010), Tofovic et al. (1998)
Q64057	Alpha-aminoadipic semi-aldehyde dehydrogenase (ALDH)	2.083	0.05	Multifunctional enzyme mediating important protective effects/Protects against hyperosmotic stress/Protects cells from oxidative stress by metabolizing a number of lipid peroxidation-derived aldehydes	Brocker et al. (2010)
P98158	Low-density lipoprotein receptor-related protein 2 (Lrp2)	1.786	0.03	Acts together with cubilin to mediate HDL endocytosis/down-regulation of Lrp2 protein in apical pole from kidney proximal tubule is associated with nephrosis in male rat	Russo et al. (2007)
Q5XI73	Rho GDP dissociation inhibitor alpha (ARHGDIA)	0.522	0.005	Regulates the GDP/GTP exchange reaction of the Rho proteins by inhibiting the dissociation of GDP from them, and the subsequent binding of GTP to them/knockout mouse for ARHGDIA displayed increased tubulointerstitial nephritis and degeneration of renal tubular epithelial cells	Togawa et al. (1999)
Unique proteins					
P30152	Neutrophil gelatinase-associated lipocalin (NGAL)	–	–	Iron-trafficking protein involved in multiple processes such as apoptosis, innate immunity and renal development/involved in apoptosis due to interleukin-3 (IL3) deprivation/it is a marker and predictor of renal injury/up-regulation of NGAL is associated with ischemic acute kidney injury	Trof et al. (2006)
P06762	Heme oxygenase 1 (Hmox-1)	–	–	Heme oxygenase cleaves the heme ring to form biliverdin. Biliverdin is subsequently converted to bilirubin by biliverdin reductase	Camara and Soares (2005), Zager (1996)
P01048	Rat T-kininogen 1 (Isoform 1 of LMWK)	–	–	Acute-phase inflammatory response/precursor of the active peptide bradykinin (BK)/related to vasodilation, hypotension and increase in vascular permeability/participates of the contact-phase reactions of blood coagulation and kallikrein-kinin system/*L. obliqua* venom is able to release BK from LMWK	Bohrer et al. (2007), Pinto et al. (2010)
P14480-1	Isoform 1 of Fibrinogen beta chain (FbB)	–	–	Precursor of fibrin clots/polymerize into fibrin and acting as a cofactor in platelet aggregation/conversion of fibrinogen to fibrin is triggered by thrombin/up-regulation of Fb mRNA in kidney is associated with proximal tubular injury and intra-glomerular fibrin deposition	Thukral et al. (2005)
P20961	Plasminogen activator inhibitor 1 (PAI-1)	–	–	Serine protease inhibitor. This inhibitor acts as "bait" for tissue plasminogen activator, urokinase, protein C and matriptase-3/it's the major control point in the regulation of fibrinolysis/up-regulation of PAI-1 is associated with renal thrombosis and fibrosis in cases of chronic allograft nephropathy	Revelo et al. (2005)
P50115	Protein S100-A8	–	–	Calcium- and zinc-binding protein/plays a prominent role in the regulation of inflammatory processes and immune response/its proinflammatory activity includes recruitment of leukocytes, promotion of cytokine and chemokine production, and regulation of leukocyte adhesion and migration. Can induce cell death via autophagy and apoptosis and this occurs through the cross-talk of mitochondria and lysosomes via reactive oxygen species (ROS)	Basnakian et al. (2002)

Table 2 continued

Acession number[a]	Protein description	Fold change[b]	*p* value[c]	Biological function and/or participation in disease	References
P02680-1	Gamma-B of Fibrinogen gamma chain (FbG)	–	–	Precursor of fibrin clots/polymerize into fibrin and acting as a cofactor in platelet aggregation/conversion of fibrinogen to fibrin is triggered by thrombin/up-regulation of Fb mRNA in kidney is associated with proximal tubular injury and intra-glomerular fibrin deposition	Thukral et al. (2005)
Q64268	Heparin cofactor 2 (HC-2)	–	–	Thrombin inhibitor/it is activated by the glycosaminoglycans, heparin or dermatan sulfate. In the presence of the latter, HC-II becomes the predominant thrombin inhibitor in place of antithrombin III (AT)/HC-II-levels increase in thrombosis and intravascular disseminated coagulation (DIC)	Takatsuka et al. (2006)
P84817	Mitochondrial fission 1 protein (MFP-1)	–	–	Promotes the fragmentation of the mitochondrial network and its perinuclear clustering/can induce cytochrome c release from the mitochondrion to the cytosol, ultimately leading to apoptosis. Also mediates peroxisomal fission	Basnakian et al. (2002)

Proteins functionally related to renal disease were selected and their specific role in renal pathology was reviewed based on literature data. Complete proteome analysis was included in supplemental Tables 1–3

[a] Acession number in UniProtKB/Swiss-Prot database

[b] Log(2) ratio change

[c] Spec count G test *p* value (proteins were considered differentially expressed with $p < 0.1$)

that the expression of LMWK (the main substrate of tissue kallikrein and venom kininogenases) is up-regulated in the kidneys of envenomed animals, which may favor the generation of BK. The immediate consequence of intravascular activation of KKS is a fall in systemic blood pressure and in peripheral tissues is edema and erythema formation (Bohrer et al. 2007). The participation of BK was already confirmed, since the hypotensive and edematogenic responses elicited by LOBE were inhibited by HOE-140, a B2 receptor antagonist (Bohrer et al. 2007). In agreement with these experimental observations, hypotension and reduced plasma levels of pre-kallikrein are common features observed in patients (Zannin et al. 2003), which support the evidence that KKS is activated during envenomation and is clinically relevant. Moreover, the data presented here also suggest that KKS activation may be involved in venom-induced AKI.

Tubular and glomerular alterations

Despite the scarce clinical case reports, the main pathological finding obtained from kidney biopsies is acute tubular necrosis (ATN). Experimental animals also showed histological alterations compatible with ATN such as loss of proximal brush border, cytoplasm vacuolation, pyknotic nuclei, degeneration and desquamation of necrotic cells. These necrotic cells exfoliating into the lumen due to either cell death or defective cell-to-cell or cell-to-basement membrane adhesion can obstruct the flow of filtrated fluid and give rise to a back pressure limiting glomerular filtration (Trof et al. 2006). Accordingly, in this work, markers of ATN were detected in urine (urinary γ-GT), and several proteins related to tubule injury were found to be up-regulated (Orm-1, YBX1, Alb, CK-B, FABP3 and NHE-RF1) or uniquely expressed (NGAL) in the kidneys of envenomed rats. Proteins linked to apoptosis (CytC, S100-A8 and MFP-1) were also up-regulated. The occurrence of glomerular dysfunction was evident, because envenomed rats presented massive proteinuria; serum Alb had a 2.1-fold increase in the kidneys, and a band corresponding to the molecular weight of Alb was detected in urine. In addition, our results confirm that hematuria and hemoglobinuria are predominant characteristics of *L. obliqua*-induced AKI. Indeed, the venom has strong in vitro and in vivo hemolytic activity and a phospholipase A2 responsible for this effect was already isolated (Seibert et al. 2004, 2006). Intact erythrocytes were found within the tubules forming intra-tubular casts and, as a result of intravascular hemolysis, different Hb subunits were detected in urine and kidneys. It is known that the formation of Hb deposits may be toxic to renal tubules due to heme cytotoxicity (Zager 1996). Once reabsorbed by the proximal tubular cells the heme porphyrin ring is rapidly catabolized by Hmox-1 yielding equimolar amounts

of free iron, biliverdin and carbon monoxide (Camara and Soares 2005). Free iron then up-regulates intracellular ferritin expression, a key defense mechanism against iron-induced tissue damage. However, in the presence of large amounts of Hb, the levels of released iron also increase, saturating the binding capacity of ferritin. Thus, the iron not removed by ferritin binding is able to readily accept and donate electrons and greatly facilitates free radical production (Zager 1996; Khan 2009; Zager et al. 2012). As proteins related to canonical pathways of oxidative stress were identified exclusively in the kidneys of LOBE-treated rats, we believe that heme cytotoxicity plays a significant role in *L. obliqua*-induced AKI. Consistent with this, several antioxidant enzymes (Prdx-5, Prdx-2, GST, DJ-1 and SOD) and proteins associated with heme and iron metabolism (Hmox-1, ferritin, Hpx and Cygb) were up-regulated or uniquely expressed during envenomation, suggesting that heme is effectively metabolized, generating free radicals and inducing oxidative damage to proteins, lipids and DNA. In fact, in previous experiments, we demonstrated that LOBE induces kidney DNA damage leading to double-strand breaks and formation of oxidized purines and pyrimidines (Berger et al. 2013). Probably this is associated with the increased expression of Rad50, a double-strand break repair protein, detected in the present work.

As a consequence of ATN, the excretion of Na^+ and K^+ increased significantly during envenomation. Injured proximal tubule cells have alterations in the actin and microtubule cytoskeletal networks that lead to a redistribution of Na^+/K^+ ATPase from the basolateral to the apical membrane, contributing to a decrease in Na^+ transport and reabsorption (Thadhani et al. 1996). It was reported that FE_{Na+} and FE_{K+} also increase in envenomation caused by *Bothrops* snakes (Boer-Lima et al. 1999; Linardi et al. 2011). Despite the redistribution of Na^+/K^+ ATPase to the apical membrane, Linardi et al. (2011) reported an increase in expression and activity of Na^+/K^+ ATPase during envenomation by *Bothrops alternatus* and suggest that it is a protective mechanism triggered in response to natriuresis with the aim to preserve renal function during acute damage. In agreement with this observation, we found an increase in expression of type-3 Na^+/H^+ exchanger regulatory cofactor, which is important in Na^+ and HCO_3^- reabsorption in proximal tubule cells (Trof et al. 2006). Likewise Na^+/K^+, water excretion increased significantly, and envenomed animals had polyuria. Several parameters measured, such as urinary density and osmolality, C_{osm}, C_{H2O} and FE_{H2O}, indicate that kidneys from envenomed rats are producing dilute urine through the excretion of solute-free water. Possibly, the presence of intra-tubular Na^+ not reabsorbed by proximal tubule cells may contribute to the increased water excretion and both, Na^+ and water rejection, may also be associated with the fall in blood pressure.

Regarding the glomerular dysfunctions, a valuable hypothesis that should be considered is the deposition of fibrin clots in glomerular capillaries. Indeed, the most potent activity of LOBE in vitro is the procoagulant activity (Donato et al. 1998; Veiga et al. 2003). In vivo, LOBE also causes activation of coagulation and fibrinolysis leading to a consumptive coagulopathy characteristic of this type of envenomation. Two enzymes responsible for the venom procoagulant activity, activators of prothrombin and factor X, have already been isolated (Alvarez-Flores et al. 2006; Reis et al. 2006). Besides the direct effect on coagulation factors, LOBE is also able to induce a procoagulant profile in endothelial cells in culture through an up-regulation of TF expression (Pinto et al. 2008). Confirming these results obtained in endothelial cells, envenomed kidneys showed an increase in TF procoagulant activity. In addition, the expression of known markers of disseminated intravascular coagulation and thrombosis (serpin 1 alpha-1 antiproteinase, PAI-1 and HC-2) increased in the kidneys of venom-treated rats. The gamma and beta chains of fibrinogen were detected solely in envenomed kidneys, which are probably related to the PAS-positive stain observed in glomeruli and are suggestive of fibrin formation.

Renal inflammation

Intense inflammatory response is a common feature in *L. obliqua* envenomation. Pain and edema are the most characteristic initial symptoms observed at the local site of contact (Zannin et al. 2003). Usually signs of systemic inflammation with neutrophilic leukocytosis, cell infiltrate and edema have also been described in lungs, kidney and heart of experimental animals (Berger et al. 2013). The inflammatory response is accompanied by the production of several cytokines (TNF, IL-1β IL-8, IL-6, CCL2 and CXCL1), vasoactive mediators (BK, histamine, prostaglandins and nitric oxide), adhesion molecules (E-selectin, VCAM-1 and ICAM-3) and an increase in leukocyte rolling and adhesion to the endothelium (Alvarez-Flores et al. 2006; Bohrer et al. 2007; Pinto et al. 2008; Berger et al. 2010; Nascimento-Silva et al. 2012). Specifically in the kidney, it was observed an up-regulation of several proteins related to acute-phase inflammatory signaling, nephritis, inflammatory cell infiltration, increase in vascular permeability, glomerular dilation, distention of Bowman's space and interstitial edema. Kidney sections stained with picrosirius revealed extensive collagen deposition in cortical periglomerular and peritubular regions and proteins involved with fibrosis, such as Cygb, PAI-1, complement C3 and complement factor D were identified. Enhanced deposition of extracellular matrix (ECM) proteins in renal tissue has been observed in response to a variety of stimuli, including TGF-β, TNF-α, IL-1, several adhesion molecules and

chemoattractants. These stimuli can also increase the levels of tissue inhibitors of matrix metalloproteinases, thereby attenuating ECM turnover, and thus, favoring the deposition of collagen and other matrix proteins (Eddy 1996; Pawluczyk and Harris 1998).

Besides fibrosis, activated complement components (C3 and factor D) may also contribute to the alterations in vascular permeability and acts as a chemoattractant for neutrophils (Turnberg et al. 2006). Moreover, complement activation by albumin is a powerful underlying mechanism of tubular and interstitial injury via cytotoxic, proinflammatory and fibrogenic effects, which often occur in renal diseases where proteinuria is present (Portella et al. 2013). In an experiment conducted in proximal tubular cells incubated with serum proteins, in vitro complement activation was observed, which could be associated with changes in the cytoskeleton, production of superoxide anion, hydrogen peroxide and proinflammatory cytokines, such as IL-6 and TNF-α (Abbate et al. 2006).

Direct venom cytotoxic activity

As the kidneys are highly vascularized organs, they are particularly susceptible to direct venom toxicity (Sitprija 2006). Renal epithelial cells in culture and isolated perfused kidneys have been used to characterize the direct cytotoxic effects of different venoms including bee, snake and spider venoms. The most common isolated toxins, which are nephrotoxic, belong to the classes of metalloproteinases, serine proteinases, C-type lectins, phospholipases A2, sphingomyelinases D and L-amino acid oxidases (Berger et al. 2012). In the case of *L. obliqua*, some toxins belonging to these classes have already been isolated (Pinto et al. 2010); however, their effects on renal cells are unknown. Our results provide some evidence that the whole venom probably has a direct nephrotoxic effect, since immunohistochemical staining confirmed the presence of venom in renal tissue, with stronger staining in the initial 6 h after venom administration followed by a progressive decrease thereafter. The venom was rapidly excreted in urine, because at least 5 bands which specifically react with antibodies raised against *L. obliqua* toxins were detected in urine. Interestingly, the positive immunohistochemical reaction for venom in different kidney structures agreed with the morphological and histological damage caused by the venom in these anatomical regions and indicated that there was a close correlation between the sites of venom localization and subsequent tissue injury. Previous studies are consistent with our observations. Using immunochemical and radiolabeling methods to analyze venom biodistribution in rats, the highest quantities of LOBE were detected in kidneys, blood and urine (Rocha-Campos et al. 2001; Da Silva et al. 2004).

Conclusion

In this work, a rat experimental model was used to study the progression of renal disease during *Lonomia obliqua* envenomation. According to our results, the pathophysiological mechanism involved in *L. obliqua*-induced AKI seems to be multifactorial where events such as systemic hypotension and fibrin deposition contribute to renal hypoperfusion, tubular necrosis and the sudden loss of basic renal functions, including filtration and excretion capacities, urinary concentration and maintenance of body fluid homeostasis. In addition, when compared to control rats, the kidneys from envenomed animals showed to be increasingly enriched for stress-related proteins, which are commonly associated with inflammation, tissue injury, heme-induced oxidative stress, coagulation and complement systems activation. Finally, the localization of the venom in renal tissue agreed with morphological and functional alterations, suggesting a close correlation between venom tissue levels and renal damage. Thus, the different mechanisms as well as the renal injury biomarkers identified here can be useful and guide further experiments to the discovery of alternative forms of treatment to *L. obliqua*-induced AKI.

Acknowledgments This work was supported by funding and fellowships from the Brazilian Agencies: Coordenação de Aperfeiçoamento de Pessoal de Nível Superior, Ministério da Educação, Brazil (CAPES-MEC)—Edital Toxinologia (Processo: 23038.006277/2011-85) and Conselho Nacional de Desenvolvimento Científico e Tecnológico, Ministério da Ciência e Tecnologia, Brazil (CNPq-MCT). This work was also supported by NIH Grant P41 GM103533 (to J.R.Y.). We thank Dr. Jeffrey N. Savas for his advice on the mass spectrometric analysis and for a critical reading of the manuscript.

Conflict of interest The authors declare that there are no conflicts of interest.

References

Abbate M, Zoja C, Remuzzi G (2006) How does proteinuria cause progressive renal damage? J Am Soc Nephrol 17:2974–2984

Alvarez-Flores MP, Fritzen M, Reis CV, Chudzinski-Tavassi AM (2006) Losac, a factor X activator from *Lonomia obliqua* bristle extract: its role in the pathophysiological mechanisms and cell survival. Biochem Biophys Res Commun 343:1216–1223

Ambatipudi KS, Lu B, Hagen FK, Melvin JE, Yates JR (2009) Quantitative analysis of age specific variation in the abundance of human female parotid salivary proteins. J Proteome Res 8:5093–5102

Basnakian AG, Kaushal GP, Shah SV (2002) Apoptotic pathways of oxidative damage to renal tubular epithelial cells. Antioxid Redox Signal 4(6):915–924

Berger M, Reck J Jr, Terra RM, Pinto AF, Termignoni C, Guimarães JA (2010) *Lonomia obliqua* caterpillar envenomation causes platelet hypoaggregation and blood incoagulability in rats. Toxicon 55(1):33–44

Berger M, Vieira MAR, Guimaraes JA (2012) Acute Kidney Injury Induced by Snake and Arthropod Venoms. In: Polenakovic M (ed) Renal failure—the facts. ISBN: 978953-51-0630-2, InTech-Open, Rijeka, Croatia, pp 157–186

Berger M, Beys-da-Silva W, Santi L, de Oliveira IM, Jorge PM, Henriques JAP, Driemeier D, Vieira MAR, Guimarães JA (2013) Acute *Lonomia obliqua* caterpillar envenomation-induced physiopathological alterations in rats: Evidence of new toxic venom activities and the efficacy of serum therapy to counteract systemic tissue damage. Toxicon 74:179–192

Boer-Lima PA, Gontijo JA, da Cruz-Höfling MA (1999) Histologic and functional renal alterations caused by *Bothrops moojeni* snake venom in rats. Am J Trop Med Hyg 61(5):698–706

Bohrer CB, Reck J Jr, Fernandes D, Sordi R, Guimarães JA, Assreuy J, Termignoni C (2007) Kallikrein-kinin system activation by *Lonomia obliqua* caterpillar bristles: involvement in edema and hypotension responses to envenomation. Toxicon 49:663–669

Bowler RP, Duda B, Chan ED, Enghild JJ, Ware LB, Matthay MA, Duncan MW (2004) Proteomic analysis of pulmonary edema fluid and plasma in patients with acute lung injury. Am J Physiol Lung Cell Mol Physiol 286(6):L1095–L1104

Brocker C, Lassen N, Estey T, Pappa A, Cantore M, Orlova VV, Chavakis T, Kavanagh KL, Oppermann U, Vasiliou V (2010) Aldehyde dehydrogenase 7A1 (ALDH7A1) is a novel enzyme involved in cellular defense against hyperosmotic stress. J Biol Chem 285(24):18452–18463

Burdmann EA, Antunes I, Saldanha LB, Abdulkader RC (1996) Severe acute renal failure induced by the venom of *Lonomia* caterpillars. Clin Nephrol 46(5):337–339

Caliari MV (1997) Princípios de Morfometria Digital: KS300 para iniciantes. Ed. UFMG

Camara NO, Soares MP (2005) Heme oxygenase-1 (HO-1), a protective gene that prevents chronic graft dysfunction. Free Radic Biol Med 38(4):426–435

Caplin B, Wang Z, Slaviero A, Tomlinson J, Dowsett L, Delahaye M, Salama A, Wheeler DC, Leiper J (2012) Alanine-glyoxylate aminotransferase-2 metabolizes endogenous methylarginines, regulates NO, and controls blood pressure. Arterioscler Thromb Vasc Biol 32(12):2892–2900

Carvalho PC, Fischer JS, Chen EI, Yates JR 3rd, Barbosa VC (2008) PatternLab for proteomics: a tool for differential shotgun proteomics. BMC Bioinform 9:316

Carvalho PC, Fischer JS, Xu T, Yates JR 3rd, Barbosa VC (2012) PatternLab: from mass spectra to label-free differential shotgun proteomics. Curr Protoc Bioinform Chapter 13(Unit13):19

Chandler RJ, Zerfas PM, Shanske S, Sloan J, Hoffmann V, DiMauro S, Venditti CP (2009) Mitochondrial dysfunction in mut methylmalonic acidemia. FASEB J 23(4):1252–1261

Chang SH, Phelps PC, Berezesky IK, Ebersberger ML Jr, Trump BF (2000) Studies on the mechanisms and kinetics of apoptosis induced by microinjection of cytochrome c in rat kidney tubule epithelial cells (NRK-52E). Am J Pathol 156(2):637–649

Chen G, Paka L, Kako Y, Singhal P, Duan W, Pillarisetti S (2001) A protective role for kidney apolipoprotein E: regulation of mesangial cell proliferation and matrix expansion. J Biol Chem 276:49142–49147

Chinnaiyan AM, Huber-Lang M, Kumar-Sinha C, Barrette TR, Shankar-Sinha S, Sarma VJ, Padgaonkar VA, Ward PA (2001) Molecular signatures of sepsis: multiorgan gene expression profiles of systemic inflammation. Am J Pathol 159(4):1199–1209

Da Silva GH, Panunto PC, Hyslop S, Da Cruz-Höfling MA (2004) Immunochemical detection of *Lonomia obliqua* caterpillar venom in rats. Microsc Res Tech 65:276–281

Devarajan P, Krawczeski CD, Nguyen MT, Kathman T, Wang Z, Parikh CR (2010) Proteomic identification of early biomarkers of acute kidney injury after cardiac surgery in children. Am J Kidney Dis 56(4):632–642

Dias da Silva W, Campos CM, Gonçalves LR, Sousa-e-Silva MC, Higashi HG, Yamagushi IK, Kelen EM (1996) Development of an antivenom against toxins of *Lonomia obliqua* caterpillars. Toxicon 34:1045–1049

Donato JL, Moreno RA, Hyslop S, Duarte A, Antunes E, Le Bonniec BF, Rendu F, de Nucci G (1998) *Lonomia obliqua* Caterpillar Spicules Trigger Human Blood Coagulation via Activation of Factor X and Prothrombin. Thromb Haemost 79:539–542

Duarte AC (1997) Síndrome Hemorrágica causada por larvas de mariposa do gênero Lonomia: estudo clínico-epidemiológico [Dissertação]. Universidade Federal do Rio Grande do Sul. Porto Alegre

Duarte AC, Caovilla JJ, Lorini JD, Mantovani G, Sumida J, Manfre PC, Silveira RC, de Moura SP (1990) Insuficiência renal aguda por acidentes com lagartas. J Bras Nefrol 12:184–187

Duarte AC, Crusius PS, Pires CAL (1994) Insuficiência renal aguda nos acidentes com *lonomia obliqua*. Nefrol Lat Am 1(1):38–40

Eng JK, Mccormack AL, Yates JR (1994) An approach to correlate tandem mass-spectral data of peptides with amino-acid-sequences in a protein database. J Am Soc Mass Spectrom 5(11):976–989

Eddy AA (1996) Molecular insights into renal interstitial fibrosis. J Am Soc Nephrol 7:2495–2508

Eddy AA (2004) Proteinuria and interstitial injury. Nephrol Dial Transpl 9(2):277–281

Fan HW, Cardoso JL, Olmos RD, Almeida FJ, Viana RP, Martinez AP (1998) Hemorrhagic syndrome and acute renal failure in a pregnant woman after contact with *Lonomia* caterpillars: a case report. Rev Inst Med Trop São Paulo 40(2):119–120

Feng MG, Navar LG (2010) Afferent arteriolar vasodilator effect of adenosine predominantly involves adenosine A2B receptor activation. Am J Physiol Renal Physiol 299(2):F310–F315

Gamborgi GP, Metcalf EB, Barros EJG (2006) Acute renal failure provoked by toxin from caterpillars of the species *Lonomia obliqua*. Toxicon 47:68–74

Godoy JR, Oesteritz S, Hanschmann EM, Ockenga W, Ackermann W, Lillig CH (2011) Segment-specific overexpression of redoxins after renal ischemia and reperfusion: protective roles of glutaredoxin 2, peroxiredoxin 3, and peroxiredoxin 6. Free Radic Biol Med 51(2):552–561

Guder WG, Ross BD (1984) Enzyme distribution along the nephron. Kidney Int 26:101–111

Khan FY (2009) Rhabdomyolysis: a review of the literature. Neth J Med 67(9):272–283

Klein MI, Xiao J, Lu B, Delahunty CM, Yates JR 3rd, Koo H (2012) *Streptococcus mutans* protein synthesis during mixed-species biofilm development by high-throughput quantitative proteomics. PLoS One 7:e45795

Laemmli UK (1970) Cleavage of structural proteins during the assembly of the head of bacteriophage T4. Nature 227:680–685

Larsen R, Gozzelino R, Jeney V, Tokaji L, Bozza FA, Japiassú AM, Bonaparte D, Cavalcante MM, Chora A, Ferreira A, Marguti I, Cardoso S, Sepúlveda N, Smith A, Soares MP (2010) A central role for free heme in the pathogenesis of severe sepsis. Sci Transl Med 2(51):51ra71

Linardi A, Rocha e Silva TA, Miyabara EH, Franco-Penteado CF, Cardoso KC, Boer PA, Moriscot AS, Gontijo JA, Joazeiro PP, Collares-Buzato CB, Hyslop S (2011) Histological and functional renal alterations caused by *Bothrops alternatus* snake venom: expression and activity of Na+/K+-ATPase. Biochim Biophys Acta 1810(9):895–906

McDonald WH, Tabb DL, Sadygov RG, MacCoss MJ, Venable J, Graumann J, Johnson JR, Cociorva D, Yates JR (2004) MS1, MS2, and SQT-three unified, compact, and easily parsed file formats for the storage of shotgun proteomic spectra and identifications. Rapid Commun Mass Spectrom 18(18):2162–2168

Morrissey JH (1995) Tissue factor modulation of factor VIIa activity: use in measuring trace levels of factor VIIa in plasma. Thromb Haemost 74(1):185–188

Mimura I, Nangaku M, Nishi H, Inagi R, Tanaka T, Fujita T (2010) Cytoglobin, a novel globin, plays an antifibrotic role in the kidney. Am J Physiol Renal Physiol 299(5):F1120–F1133

Nascimento-Silva V, Rodrigues da Silva G, Moraes JA, Cyrino FZ, Seabra SH, Bouskela E, Almeida Guimarães J, Barja-Fidalgo C (2012) A pro-inflammatory profile of endothelial cell in *Lonomia obliqua* envenomation. Toxicon 60(1):50–60

Nishi H, Inagi R, Kawada N, Yoshizato K, Mimura I, Fujita T, Nangaku M (2011) Cytoglobin, a novel member of the globin family, protects kidney fibroblasts against oxidative stress under ischemic conditions. Am J Pathol 178(1):128–139

Pawluczyk IZA, Harris KPG (1998) Cytokine interactions promote synergistic fibronectin accumulation by mesangial cells. Kidney Int 54:62–70

Peng J, Elias JE, Thoreen CC, Licklider LJ, Gygi SP (2003) Evaluation of multidimensional chromatography coupled with tandem mass spectrometry (LC/LC-MS/MS) for large-scale protein analysis. The yeast proteome. J Proteome Res 2:43–50

Pinho FM, Zanetta DM, Burdmann EA (2005) Acute renal failure after *Crotalus durissus* snakebite: a prospective survey on 100 patients. Kidney Int 67(2):659–667

Pinto AFM, Silva KRLM, Guimaraes JA (2006) Proteases from *Lonomia obliqua* venomous secretions: comparison of procoagulant, fibrin(ogen)olytic and amidolytic activities. Toxicon 47:113–121

Pinto AFM, Dragulev B, Guimarães JA, Fox JW (2008) Novel perspectives in the pathogenesis of *Lonomia obliqua* caterpillar envenomation based on assessment of host response by gene expression analysis. Toxicon 51:1119–1128

Pinto AFM, Berger M, Reck-Jr J, Terra RM, Guimarães JA (2010) *Lonomia obliqua* venom: *In vivo* effects and molecular aspects associated with the hemorrhagic syndrome. Toxicon 56(7):1103–1112

Portella VG, Silva-Filho JL, Landgraf SS, de Rico TB, Vieira MA, Takiya CM, Souza MC, Henriques MG, Canetti C, Pinheiro AA, Benjamim CF, Caruso-Neves C (2013) Sepsis-surviving mice are more susceptible to a secondary kidney insult. Crit Care Med 41(4):1056–1068

Pompermayer K, Souza DG, Lara GG, Silveira KD, Cassali GD, Andrade AA, Bonjardim CA, Passaglio KT, Assreuy J, Cunha FQ, Vieira MA, Teixeira MM (2005) The ATP-sensitive potassium channel blocker glibenclamide prevents renal ischemia/reperfusion injury in rats. Kidney Int 67(5):1785–1796

Reis CV, Andrade SA, Ramos OH, Ramos CR, Ho PL, Batista IF, Chudzinski-Tavassi AM (2006) Lopap, a prothrombin activator from *Lonomia obliqua* belonging to the lipocalin family: recombinant production, biochemical characterization and structure-function insights. Biochem J 398(2):295–302

Revelo MP, Federspiel C, Helderman H, Fogo AB (2005) Chronic allograft nephropathy: expression and localization of PAI-1 and PPAR-gamma. Nephrol Dial Transpl 20:2812–2819

Ricci-Silva ME, Valente RH, León IR, Tambourgi DV, Ramos OH, Perales J, Chudzinski-Tavassi AM (2008) Immunochemical and proteomic technologies as tools for unravelling toxins involved in envenoming by accidental contact with *Lonomia obliqua* caterpillars. Toxicon 51:1017–1028

Rocha-Campos AC, Gonçalves LR, Higasshi HG, Yamagushi IK, Fernandes I, Oliveira JE, Ribela MT, Sousa-e-Silva MC, Dias da Silva W (2001) Specific heterologous F(ab')2 antibodies revert blood incoagulability resulting from envenoming by *Lonomia obliqua* caterpillars. Am J Trop Med Hyg 64:283–289

Russo LM, Sandoval RM, McKee M, Osicka TM, Collins AB, Brown D, Molitoris BA, Comper WD (2007) The normal kidney filters nephrotic levels of albumin retrieved by proximal tubule cells: retrieval is disrupted in nephrotic states. Kidney Int 71(6):504–513

Safadi FF, Thornton P, Magiera H, Hollis BW, Gentile M, Haddad JG, Liebhaber SA, Cooke NE (1999) Osteopathy and resistance to vitamin D toxicity in mice null for vitamin D binding protein. J Clin Invest 103(2):239–251

Schrier RW, Wang W, Poole B, Mitra A (2004) Acute renal failure: definitions, diagnosis, pathogenesis, and therapy. J Clin Invest 114(1):5–14

Seibert CS, Oliveira MRL, Gonçalves LRC, Santoro ML, Sano-Martins IS (2004) Intravascular hemolysis induced by *Lonomia obliqua* caterpillar bristle extract: an experimental model of envenomation in rats. Toxicon 44:793–799

Seibert CS, Tanaka-Azevedo AM, Santoro ML, Mackessy SP, Torquato RJS, Lebrun I, Tanaka AS, Sano-Martins IS (2006) Purification of a phospholipase A_2 from *Lonomia obliqua* caterpillar bristle extract. Biochem Biophys Res Commun 342:1027–1033

Shashidharamurthy R, Mahadeswaraswamy YH, Ragupathi L, Vishwanath BS, Kemparaju K (2010) Systemic pathological effects induced by cobra (Naja naja) venom from geographically distinct origins of Indian peninsula. Exp Toxicol Pathol 62(6):587–592

Sitprija V (2006) Snakebite nephropathy. Nephrology (Carlton) 11(5):442–448

Son D, Kojima I, Inagi R, Matsumoto M, Fujita T, Nangaku M (2008) Chronic hypoxia aggravates renal injury via suppression of Cu/Zn-SOD: a proteomic analysis. Am J Physiol Renal Physiol 294(1):F62–F72

Stefanska B, Huang J, Bhattacharyya B, Suderman M, Hallett M, Han ZG, Szyf M (2011) Definition of the landscape of promoter DNA hypomethylation in liver cancer. Cancer Res 71(17):5891–5903

Tabb DL, McDonald WH, Yates JR 3rd (2002) DTASelect and Contrast: tools for assembling and comparing protein identifications from shotgun proteomics. J Proteome Res 1:21–26

Takatsuka H, Nakajima T, Nomura K, Wakae T, Toda A, Itoi H, Okada M, Misawa M, Hara H (2006) Heparin cofactor II as a predictor of thrombotic microangiopathy after bone marrow transplantation. Hematology 11(2):101–103

Thadhani R, Pascual M, Bonventre JV (1996) Acute renal failure. N Engl J Med 334(22):1448–1460

Thukral SK, Nordone PJ, Hu R, Sullivan L, Galambos E, Fitzpatrick VD, Healy L, Bass MB, Cosenza ME, Afshari CA (2005) Prediction of nephrotoxicant action and identification of candidate toxicity-related biomarkers. Toxicol Pathol 33(3):343–355

Tofovic SP, Kusaka H, Li P, Jackson EK (1998) Effects of adenosine deaminase inhibition on blood pressure in old spontaneously hypertensive rats. Clin Exp Hypertens 20(3):329–344

Togawa A, Miyoshi J, Ishizaki H, Tanaka M, Takakura A, Nishioka H, Yoshida H, Doi T, Mizoguchi A, Matsuura N, Niho Y, Nishimune Y, Nishikawa SI, Takai Y (1999) Progressive impairment of kidneys and reproductive organs in mice lacking Rho GDIalpha. Oncogene 18(39):5373–5380

Trof RJ, Di Maggio F, Leemreis J, Groeneveld AB (2006) Biomarkers of acute renal injury and renal failure. Shock 26(3):245–253

Turnberg D, Lewis M, Moss J, Xu Y, Botto M, Cook HT (2006) Complement activation contributes to both glomerular and tubulointerstitial damage in adriamycin nephropathy in mice. J Immunol 177:4094–4102

Veiga ABG, Blochtein B, Guimarães JA (2001) Structures involved production, secretion and injection of the venom produced by the caterpillar *Lonomia obliqua* (Lepidoptera, saturniidae). Toxicon 39:1343–1351

Veiga ABG, Pinto AFM, Guimarães JA (2003) Fibrinogenolytic and procoagulant activities in the hemorrhagic syndrome caused by *Lonomia obliqua* caterpillars. Thromb Res 111(1–2):95–101

Veiga ABG, Ribeiro JM, Guimarães JA, Francischetti IM (2005) A catalog for the transcripts from the venomous structures of the

caterpillar *Lonomia obliqua*: identification of the proteins potentially involved in the coagulation disorder and hemorrhagic syndrome. Gene 355:11–27

Warrell DA (2010) Snake bite. Lancet 375(9708):77–88

Washburn MP, Wolters D, Yates JR 3rd (2001) Large-scale analysis of the yeast proteome by multidimensional protein identification technology. Nat Biotechnol 19:242–247

Williams D, Gutiérrez JM, Harrison R, Warrell DA, White J, Winkel KD, Gopalakrishnakone P (2010) Global snake bite initiative working group; international society on toxinology. The global snake bite initiative: an antidote for snake bite. Lancet 375(9708):89–91

Xu T, Venable JD, Park SK, Cociorva D, Lu B (2006) ProLuCID, a fast and sensitive tandem mass spectra-based protein identification program. Mol Cell Proteomics 5:S174

Zager RA (1996) Rhabdomyolysis and myohemoglobinuric acute renal failure. Kidney Int 49(2):314–326

Zager RA, Johnson AC, Becker K (2012) Renal cortical hemopexin accumulation in response to acute kidney injury. Am J Physiol Renal Physiol 303(10):F1460–F1472

Zannin M, Lourenço DM, Motta G, Costa LRD, Grando M, Gamborgi GP, Noguti MA, Chudzinski-Tavassi AM (2003) Blood coagulation and fibrinolytic factors in 105 patients with hemorrhagic syndrome caused by accidental contact with *Lonomia obliqua* caterpillar in Santa Catarina, Southern Brazil. Thromb Haemost 89:355–364